# UNIVERSITI TEKNOLOGI MALAYSIA

## BORANG PENGESAHAN
## LAPORAN AKHIR PENYELIDIKAN

TAJUK PROJEK : The Study on the Development of Saturation Profile in Soil Slope

Saya ASSOC. PROF. DR. NURLY GOFAR
**(HURUF BESAR)**

Mengaku membenarkan **Laporan Akhir Penyelidikan** ini disimpan di Perpustakaan Universiti Teknologi Malaysia dengan syarat-syarat kegunaan seperti berikut :

1. Laporan Akhir Penyelidikan ini adalah hakmilik Universiti Teknologi Malaysia.
2. Perpustakaan Universiti Teknologi Malaysia dibenarkan membuat salinan untuk tujuan rujukan sahaja.
3. Perpustakaan dibenarkan membuat penjualan salinan Laporan Akhir Penyelidikan ini bagi kategori TIDAK TERHAD.
4. * Sila tandakan ( / )

| | | |
|---|---|---|
| ☐ | SULIT | (Mengandungi maklumat yang berdarjah keselamatan atau Kepentingan Malaysia seperti yang termaktub di dalam AKTA RAHSIA RASMI 1972). |
| ☐ | TERHAD | (Mengandungi maklumat TERHAD yang telah ditentukan oleh Organisasi/badan di mana penyelidikan dijalankan). |
| ☑ | TIDAK TERHAD | |

TANDATANGAN KETUA PENYELIDIK
DR. NURLY GOFAR
Associate Professor (DS53)
Department of Geotechnics & Transportation
Faculty of Civil Engineering
Universiti Teknologi Malaysia
Nama & Cop Ketua Penyelidik

Tarikh: 31 Julai 2008

CATATAN : **Jika Laporan Akhir Penyelidikan ini SULIT atau TERHAD, sila lampirkan surat daripada pihak berkuasa/ organisasi berkenaan dengan menyatakan sekali sebab dan tempoh laporan ini perlu dikelaskan sebagai SULIT dan TERHAD.*

VOT 78152

# THE STUDY ON THE DEVELOPMENT OF SATURATION PROFILE IN SOIL SLOPE

# (KAJIAN MENGENAI PERKEMBANGAN PROFIL KETEPUAN DALAM TANAH CERUN)

**NURLY GOFAR**
**LEE MIN LEE**

**FAKULTI KEJURUTERAAN AWAM**
**UNIVERSITI TEKNOLOGI MALAYSIA**

**2008**

# ACKNOWLEDGEMENT

We would like to thank Universiti Teknologi Malaysia for funding the research through Initial Research Grant Scheme for Students (IRGS). This research would not be accomplished without the financial aids provided.

The research was shaped through interaction with many academicians. For this, we are deeply grateful to Professor Dr. Harianto Rahardjo, Dr. David Toll, Professor Dr. Roslan Zainal Abidin, Professor Dr. Faisal Ali, Professor Dr. Mohd Amin Mohd Sam, and Mr. Low Tian Huat for sharing their valuable experiences.

We extend our gratitude to all the technical staffs of Department of Geotechnics and Transportation, Faculty of Civil Engineering, Universiti Teknologi Malaysia for their assistance in laboratory and field works. Besides, we sincerely thank fellow Master and Undergraduate students including Mohamed Elbyhagi, Wisam, Maiziz, Amir Hasyim, Sim Kay Huei, Tan She Hooi, Yang Eik Hien, Elango, and Nadasan, for their involvement in part of this research.

## ABSTRACT

This study was carried out to investigate the mechanisms involved in the development of saturation profiles in soil. A series of laboratory tests were conducted to monitor the saturation profiles in four types of soil under various rainfall conditions. The understanding in saturation profile is essential to predict the shear strength of soil, particularly for slope stability problem. The study showed that the saturation profile in soil could be effectively monitored through a fabricated soil column model. The effect of rainfall pattern on the saturation profile of coarse-grained soil is relatively insignificant. Conversely, the saturation profile in fine-grained soil could be significantly altered when the soil is subjected to a prolonged rainfall. It is believed that the findings from the present study could lead to better understanding of saturation profile in soil, and subsequently contributing efforts in mitigating rainfall-induced slope failure.

# ABSTRAK

Kajian ini dijalankan untuk mengkaji mekanisme yang terlibat dalam perkembangan profil ketepuan dalam tanah. Satu siri ujian makmal telah dijalankan untuk memantau profil ketepuan empat jenis tanah dalam pelbagai keadaan hujan. Kefahaman dalam profil ketepuan adalah penting untuk meramal kekuatan tanah terutamanya bagi masalah kestabilan cerun. Kajian ini menunjukkan profil ketepuan tanah dapat dimantau dengan efektifnya dengan menggunakan satu model tiang tanah. Kesan corak hujan terhadap profil ketepuan tanah berbutiran kasar didapati kurang ternyata. Sebaliknya, profil ketepuan dalam tanah berbutiiran halus berubah dengan banyak apabila tanah terdedah kepada hujan yang berpanjangan. Adalah diharapkan bahawa penemuan daripada kajian ini dapat memberi kefahaman yang lebih mendalam mengenai profil ketepuan tanah, dan seterusnya memberi sumbangan dalam pencegahan tanah runtuh akibat hujan.

# TABLE OF CONTENTS

# LIST OF TABLES

# LIST OF FIGURES

# LIST OF SYMBOLS

| | | |
|---|---|---|
| $A_{ev}$ | - | Air entry value |
| $I$ | - | Rainfall intensity |
| $k$ | - | Water coefficient of permeability |
| $k_{sat}$ | - | Saturated permeability |
| $L_f$ | - | Wetting front depth |
| $m_w$ | - | Slope of soil water characteristic curve (SWCC) |
| $q$ | - | Rainfall unit flux |
| $Q$ | - | Rainfall total flux |
| $S$ | - | Wetting front capillary suction |
| $S_r$ | - | Degree of saturation |
| $t$ | - | Time |
| $t_p$ | - | Time when surface runoff start to occur |
| $\theta$ | - | Volumetric water content |
| $\psi$ | - | Suction |

# LIST OF APPENDICES

# CHAPTER 1

# INTRODUCTION

## 1.1 Background of the Study

The stability of a slope is greatly affected by the saturation profile of soil beneath the slope. The saturation profile, in turn, is governed by several parameters such as rainfall pattern, interface boundary conditions, soil types, and its hydraulic properties. Effect of each parameter has been studied based on numerical simulations and field test. These studies were limited in term of validity and the extent of the study area.

Several field studies on the saturation and suction profile can be traced. For instance, Gasmo *et al.* (1999) described the details of the instrumentation for pore water pressure monitoring in an unsaturated residual soil slope in Singapore. In the study on the infiltration characteristics of the slope, Tsaparas *et al.* (2002) found that the changes in pore water pressure were affected by the total rainfall and the initial conditions of the slope. Li *et al.* (2005), based on a full scale field experiment on an instrumented slope in Hong Kong concluded that the propagation of wetting front was limited to the top 3 m of soil and the movements of wetting front varies with rainfall pattern. Hence, it can be concluded that most of the field studies considered the rainfall pattern as the main variable.

The effect of soil type on the saturation profile has been studied numerically by several researchers, i.e. Tsaparas *et al.* (2002), Pradel and Raad (1993), Cai and Ugai (2004) and Gofar *et al*. (2007). Most of the studies suggested that the soil with low permeability should contribute to higher degree of saturation compared to high permeable soil. Apparently, more variables can be taken into account, owing to the rapid development in computing power and numerical analyzing tools. However, the validity of the result becomes a major concern as the soil could behave differently in actual condition.

This research looked into several variables affecting the development of saturation profile, including rainfall pattern, soil type and boundary conditions. The ability to combine those parameters into a comprehensive laboratory model enhanced the understanding on the saturation profile beneath a soil slope.

## 1.2 Objectives

The study was carried out in fulfillment of the following objectives:

i. To fabricate a small scale laboratory model for investigation of the mechanisms involved in the development of saturation profile.

ii. To study the dominant factors affecting each mechanism.

iii. To study the overall mechanism in the comprehensive laboratory model

## 1.3 Scope of the Study

The study focuses mainly on laboratory modeling. A soil column model was fabricated to simulate the one-dimensional infiltration model. Monitoring instruments with automated data acquisition system were installed on the model to allow continuous pore-water pressure measurements.

Due to the constraints of the experimental apparatus and research scope, the study was exposed to certain assumptions and limitations: (1) The ideal environment in the laboratory with controlled precipitation and room temperature was assumed to be representative of the actual climate condition. (2) The infiltration rate was derived from the difference between rainfall and runoff rate. Other surface losses was assumed to be negligible. (3) The study was valid for one dimensional analysis, thus only the vertical flow was concerned. (4) The soil materials used in the numerical simulation and laboratory modeling are assumed to be homogeneous.

## 1.4 Significance of the Study

With regards to the importance of this research, the findings may be viewed as a fundamental research. The benefits that would be gained from the study include the understanding of the saturation profile for different combinations of soil types, boundary conditions, and rainfall patterns, as well as the understanding of the relationship between saturation profile and slope stability.

# CHAPTER 2

# LITERATURE STUDY

## 2.1 Introduction

This chapter provides the basic and clinical researches on the topic of saturation profile in soil. Considerable literatures relevant to the topic are available. Most of the literatures were directed towards determining the saturation profile under certain rainfall condition, development of wetting front, and studies on the hydraulic properties of unsaturated soils, and case studies from different parts of the world. The one-dimensional infiltration tests carried out by previous researchers are also reviewed in the latter part of this chapter.

## 2.2 Hydraulic Properties of Soil

The hydraulic properties of soil can be attributed to water retention characteristic (soil water characteristic curve) and water coefficient of permeability (hydraulic conductivity function).

### 2.2.1 Soil Water Characteristic Curve (SWCC)

The soil water characteristic curve (SWCC), also referred to as the soil moisture retention curve, depicts the relationship between soil water content and soil water pressure potential. A typical adsorption and desorption SWCC are shown in Figure 2.1.

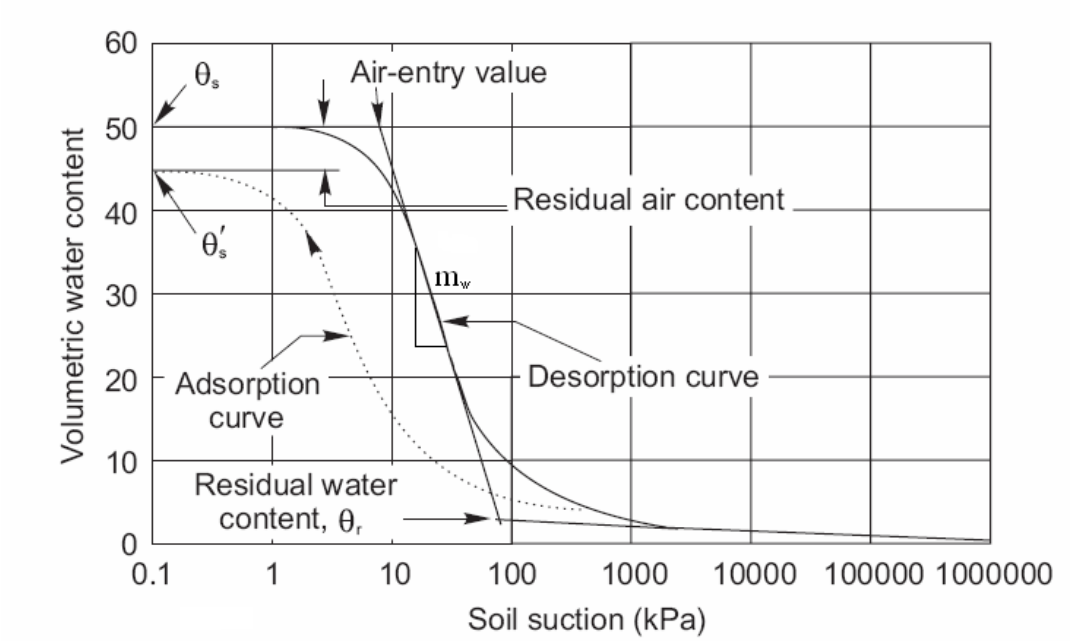


**Figure 2.1** Typical absorption and desorption SWCC (Zhan and Ng, 2004)

As observed in Figure 2.1, the volumetric water content at saturation of desorption curve ($\theta_s$) is greater than that of absorption curve ($\theta'_s$). The difference between $\theta_s$ and $\theta'_s$, defined as the residual air content, is caused by the entrapped air in the soil during absorption process. There are two characteristic points in a SWCC, namely air entry value ($A_{ev}$) and residual water content ($\theta_r$) (Zhan and Ng, 2004). The $A_{ev}$ indicates the maximum suction required to dissipate the entrapped air from the soil. Before the suction exceeds $A_{ev}$, the soil is saturated or nearly saturated, hence the behaviour of the soil is similar to that of saturated soil with a compressible fluid due to the existence of occluded air bubbles. On the other end of the curve, very little water exists in the soil when the soil suction is greater than $\theta_r$.

The effect of water content on the behaviour of soil is thus negligible. As the result, the soil at these two unsaturated stages is not the main concern for the behaviour of unsaturated soil (Bao *et al*., 1998). What is of greater concern is the SWCC between $A_{ev}$ and $\theta_r$, in which both air and water phases are continuous or partially continuous, and the soil properties are strongly related to its water content or negative pore-water pressure (Zhan and Ng, 2004). The rate of changes in negative pore-water pressure corresponding to volumetric water content is represented by the slope of SWCC ($m_w$).

A wide-array of methods can be used to obtain the SWCC, depending on the desired path (absorption or desorption) and the range of matric suction. Laboratory SWCC test can be conducted by using pressure plate test (for suction less than 1500 kPa), salt solution method (for suction greater than 1500 kPa), and capillary rise open tube method (for absorption SWCC), while field SWCC can be obtained by taking the field measurements of water content and suction by moisture probe and tensiometer, simultaneously. Alternatively, the SWCC can be predicted by using empirical relationships, as proposed by several researchers included Fredlund and Xing (1994), Agus *et al*. (2001) and Gitirana and Fredlund (2004).

### 2.2.2 Hydraulic Conductivity Function

The water coefficient of permeability ($k$) represents the soil's ability to transmit and drain water. This, in turn, indicates the ability of the soil to change matric suction as a result of environmental changes (Fredlund and Rahardjo, 1993). Water coefficient of permeability of saturated soil is a function of void ratio ($e$) only. For unsaturated soil, the water coefficient of permeability is a function of void ratio ($e$) and volumetric water content ($\theta$). This relationship is commonly expressed by a

suction-dependent hydraulic conductivity function, as illustrated in Figure 2.2.

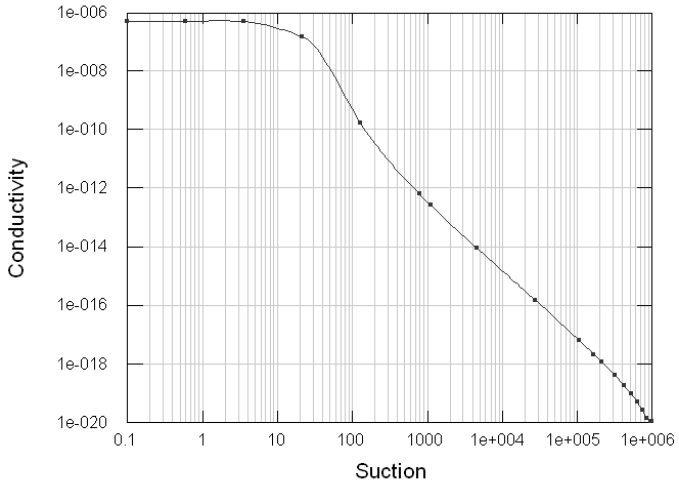


**Figure 2.2** Typical suction-dependent hydraulic conductivity function

The hydraulic conductivity function of unsaturated soil can be obtained through direct or indirect measurement. The direct measurement of unsaturated flow behaviour that commonly conducted by using Instantaneous Profile Method (IPM) is not encouraged in practice since the test requires elaborate equipment and qualified personnel, which proves time consuming and expensive (Brisson *et al.*, 2002). The duration of the test increases as the water content in the soil decreases (Leong and Rahardjo, 1997).

The indirect prediction methods for hydraulic conductivity function have been proposed by several researchers. Van Genuchten (1980) developed a close form equation to estimate unsaturated hydraulic conductivity through three independent parameters obtained by fitting the proposed soil water retention model to experimental data. The unsaturated hydraulic conductivity was predicted well in four out of five study cases. Fredlund *et al.* (1994) and Gribb *et al.* (2004) suggested that hydraulic conductivity function can be estimated through saturated permeability and SWCC by using fitting method. Leong and Rahardjo (1997) compared the hydraulic conductivity function estimated from several empirical equations, macroscopic models and statistical models. They concluded that the use

of newly developed empirical equations could give a good fit to the experimental data. In conclusion, methods of predicting hydraulic conductivity function indirectly can be used with confidence when no experimental data are feasible.

## 2.3 Rainfall Infiltration Model

Studies of rainfall infiltration have been performed systematically since the 1970s (Sung and Seung, 2002). From the definitions, the rainfall may be separated into four components, i.e. runoff, infiltration, interception (rainfall that is caught on the vegetation surfaces), and evapotranspiration (ET). Interception and ET are often disregarded when identifying rainfall components because they represent a small portion of the total rainfall (Joel *et al.* 2002). These simplifications leave the approximation of rainfall is nearly equal to the infiltration and runoff.

One of the earliest physical infiltration models was developed by Green and Ampt (1911). Based on the model, the time ($t$) required to saturate the soil to a depth ($L_f$) is:

$$t = \frac{\mu}{k_w}\left[ L_f - S\ln\left(\frac{S + L_f}{S}\right)\right] \qquad (2.1)$$

Where, $\mu$ = differences between the volumetric water content before and after wetting

$k_w$ = hydraulic conductivity of wetted zone

$S$ = wetting front capillary suction

The infiltration rate ($I_f$) is the rate at which water enter the soil surface. The Green-Ampt model predicts:

$$I_f = k_w \frac{S + L_f}{L_f} \tag{2.2}$$

In Green and Ampt's model of infiltration, water from precipitation is assumed to enter the soil as a sharp wetting front. The soil above the front is assumed to be saturated. The soil below of the front is assumed at some uniform initial moisture. This model gives a very reasonable prediction even when compared with other more rigorous approaches based on unsaturated flow (Bouwer, 1966). Other researchers such as Mein and Larson (1973), Neuman (1976), Loáiciga and Huang (2007) have produced a similar infiltration equation with some modifications.

Figure 2.3 shows the relationship between rainfall and infiltration. Initially the infiltrability ($I_p$) is greater than the rainfall intensity ($I$). Thus, the infiltration rate ($I_f$) is limited by the $I$. After a period of constant rainfall, the $I_p$ decreases over time to a rate of less than $I$. At this stage, the $I_f$ is controlled by the $I_p$, and surface runoff takes place. Horton (1933) found that when there is plenty of water available for infiltration, the infiltration rate follows the limiting function of $I_p$, until a constant rate known as infiltration capacity is reached. Freeze and Cherry (1979) found that the infiltration capacity is equal to the saturated permeability of soil ($k_{sat}$). This finding was supported by Mein and Larson (1973) who found that the infiltration rate is initially exceeded the saturated permeability of soil, but drops to a value identical to the saturated permeability when the soil becomes fully saturated.

One of the often heard questions is how long after a constant rainfall intensity will initiate the generation of surface runoff. As shown in Figure 2.3, $t_p$ is the time when surface runoff start to occur. Mein and Larsson (1973) found that $t_p$ can be predicted from an empirical equation as follows:

$$t_p = \frac{S\mu k_w}{I(I - k_w)} \tag{2.3}$$

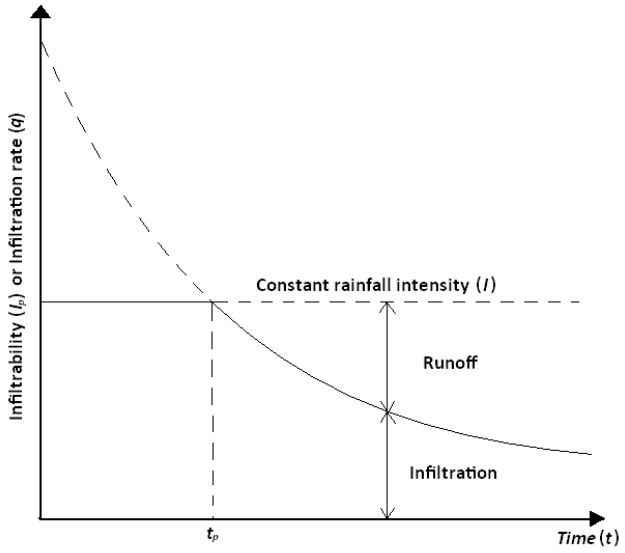


**Figure 2.3** Relationship between rainfall and infiltration

In actual condition, the infiltration-runoff system sustains much more complexity than those expressions in a simple physical or empirical model. The infiltration rate could be affected by the distribution of rainfall, soil initial condition, rearrangement of soil particles due to the impact of raindrops, swelling of clayey soils, activities of worms and other soil fauna etc. (Bouwer 1966). The simulation of infiltration process as result of a rainfall event is still possible. However, the threshold rainfall for a slope failure could be a combination of a number of rainfall events or a prolonged antecedent rainfall. Under such circumstances, the simulation of rainfall infiltration could be extremely time consuming if not impossible. Ng *et*

*al.* (2003) who carried out their studies on the rainfall-induced slope failure in Hong Kong suggested that, on average, 40% of rainfall considered as surface loss. Rahardjo *et al.* (2004) made another assumption in Singapore by suggesting 60% of rainfall contributed to the surface loss. Despite of the fact that such correlation could be vague, it is still an acceptable assumption in practice.

## 2.4 Wetting Front and Redistribution

Wetting front and redistribution are two important phenomena in the saturation profile of unsaturated soil. As mentioned earlier, the conceptual model based on a sharp wetting front approach was first developed by Green and Ampt (1911). The studies in wetting front have been extended by numerous researchers, with the likes of Lumb (1962), Bouwer (1966), Mein and Farrel (1974), Pradel and Raad (1993), Kim *et al.* (2006), and Wang *et al.* (2003). Recent studies attempted to correlate the wetting front with the redistribution in order to provide a more comprehensive explanation to the soil moisture movement after the infiltration processes (Youngs, 1958; Jury *et al.*, 2003; Wang *et al.*, 2003).

As illustrated in Figure 2.4, the wetting front depth ($L_f$) under uniform amount of rainfall infiltration ($P$) can be approximated to:

$$L_f = \frac{P}{\theta_a - \theta_i} \tag{2.4}$$

Where $\theta_a$ is the average moisture content in the wetted zone, and $\theta_i$ is the initial moisture content (Wang *et al.*, 2003).

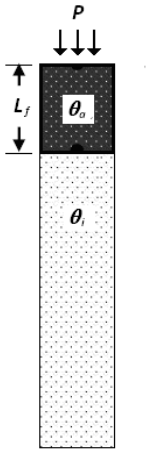


**Figure 2.4** Development of wetting front

From the absorption and desorption SWCC shown in Figure 2.5, Wang *et al.* (2003) found that the soil below the wetting front initially takes up moisture following an absorption curve OA until the suction reaches the water entry value ($W_{ev}$) at the wetting front. Subsequently, the volumetric water content increases abruptly to $\theta'_s$. Above the wetting front (soil near the ground surface), water drains out from the soil following the desorption curve BO. When the suction reaches the air-entry value ($A_{ev}$), the major pores begin to empty. The difference between the $W_{ev}$ and $A_{ev}$ indicates the ability of a porous medium to entrap a zone of higher water content behind the wetting front (Glass *et al.*, 1989). Considering the inclination angle of slope ($\beta$), Wang *et al.* (2003) revised this special moisture retention ability and proposed a term known as the critical wetting front depth ($L_{cr}$):

$$L_{cr} = \frac{W_{ev} - A_{ev}}{\cos\beta} \tag{2.5}$$

The term of critical wetting front depth was given because it is the limit for the redistribution and unstable flow to take place. In other words, when $L_f < L_{cr}$, the downward flux is not possible and the corresponding suction redistribution will be as shown in Figure 2.6a. Otherwise ($L_f > L_{cr}$), downward flow continues after water

input stops due to excessive amount of infiltration and the corresponding suction redistribution is as illustrated in Figure 2.6b. It can be inferred from recent studies that with this type of redistribution pattern, a threshold water-entry pressure at the wetting front is required for the water to enter the unwetted zone (Liu *et al.*, 1993; Geiger and Durnford, 2000).

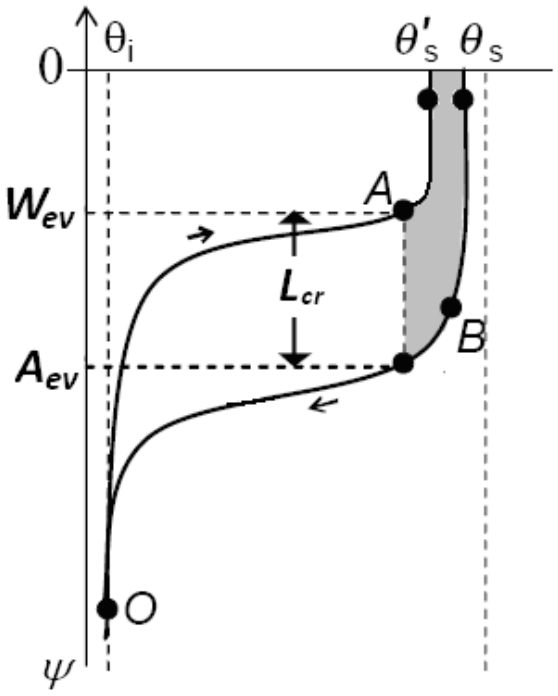


**Figure 2.5** Volumetric water content and suction in the development of wetting front

(a) (b)

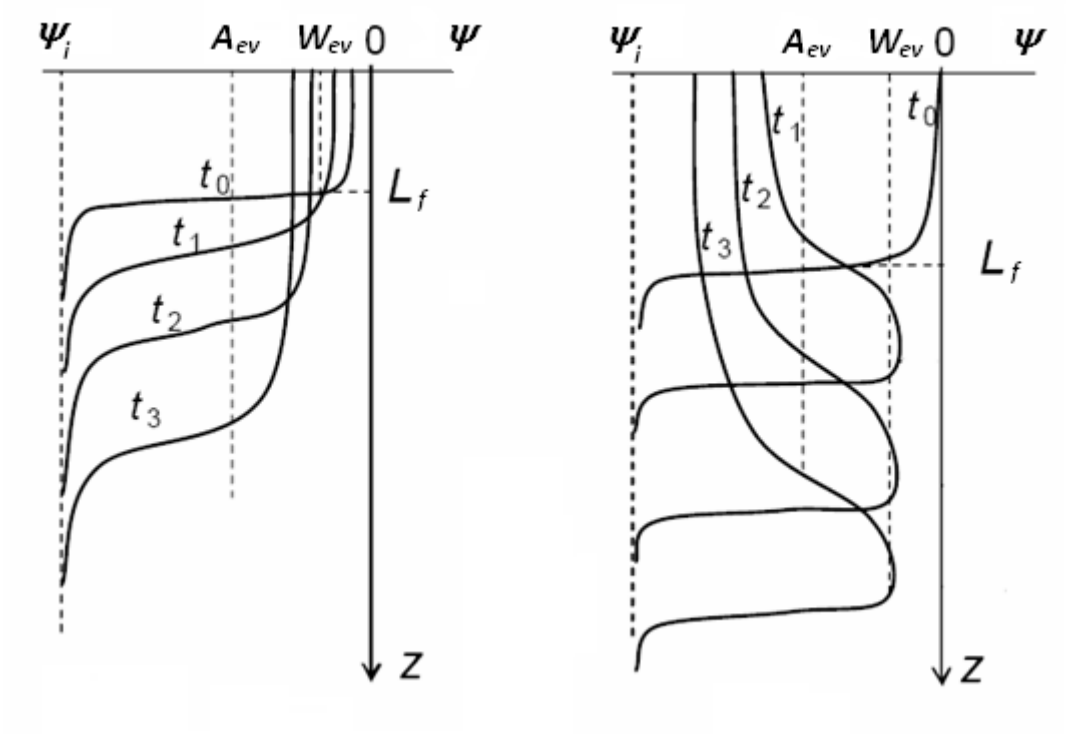


**Figure 2.6** Redistribution of soil moisture for (a) $L_f < L_{cr}$ and (b) $L_f > L_{cr}$

## 2.5 One-Dimensional Infiltration Test

Soil column has been used by several researchers to model the one-dimensional infiltration mechanism. Stormont and Anderson (1999) used a soil column apparatus to study the infiltration behavior of layered soils. The apparatus consists of an acrylic cylinder of 203 mm in diameter and 800mm in height. Nahlawi *et al.* (2007) carried out an infiltration experiment to study the one-dimensional unsaturated hydraulic behaviour of a layered soil-geotextile system. Their infiltration experiments were conducted in a clear Perspex cylinder of 138.7 mm in diameter and 1,600 mm in height. The column assembly comprises four-part cylindrical sections, with each section having a 400 mm height. Other published works on infiltration testing using one-dimensional soil column include Rousseau and Pietro (2004), Jason and Joel (2004) and Hincapié *et al.* (2007). Their studies

mainly focused on the investigation of the transportation of contaminants, chemical solutes and leachate in soil.

The modeling of infiltration mechanism by the soil column infiltration test can be traced from the studies conducted by Yang *et al*. (2004b) and Yang *et al.* (2006). Yang *et al.* (2006) investigated the effect of rainfall intensity and duration on infiltration mechanism through a large scale soil column apparatus, and provide experimental evidence for soil water redistribution and hysteresis. The details and the performance of the apparatus are described by Yang *et al*. (2004b).

Figure 2.7 shows the schematic diagram of the soil column apparatus developed by Yang *et al.* (2004b). The soil column was made of acrylic and supported by a steel frame. The soil column was 1.5m in height with the internal diameter of 190mm. Two types of instruments were installed on the soil column model, i.e. tensiometer for suction measurement, and TDR for volumetric water content measurement. The measurements were logged automatically into a data logger. Water circulation system was installed to circulate the water discharged during the tests.

A few criteria should be considered in the design of soil column model to accommodate the requirements of specific research, i.e. the dimension, the material and the boundary conditions of the model. Generally, it is recommended that the diameter of the soil column is ten times greater than the soil particle size in order to minimize the boundary effect on the test results. Lim *et al.* (1996) measured the pore-water pressure changes during rainfall in a slope in Singapore and concluded that the pore-water pressure changes occurred within the depths of 1.5m. It is thus essential to use a soil column with sufficient length and dimensions for pore-water pressure monitoring. Besides, the boundary conditions of the soil column should also be properly defined to represent the desired condition.

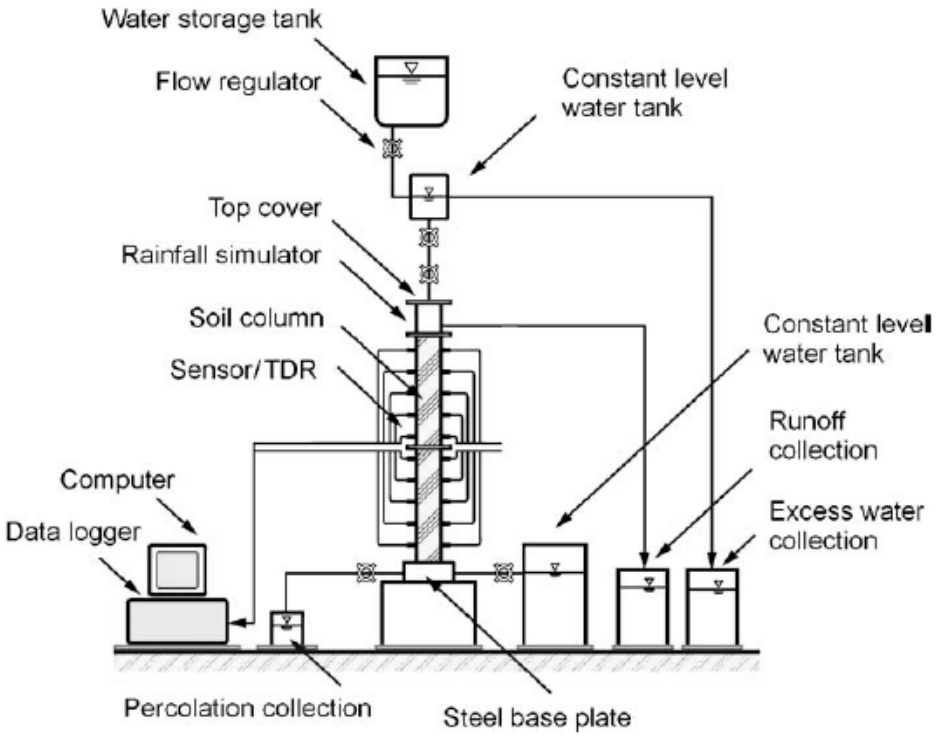


**Figure 2.7** Schematic diagram of soil column developed by Yang *et al.* (2004)

## 2.6 Concluding Remarks

In this chapter, the basic theories and the clinical researches relevant to the topic of saturation profile in soil were discussed in details. Besides, the published works related to the one-dimensional infiltration test were reviewed to provide supportive information for the methodology employed in the present study.

Despite of the fact that the theory of soil infiltration has been well established, the factor affecting the saturation profile in soil is still unclear. Both soil properties and rainfall characteristics could govern the saturation profile. However, which factors are dominating the mechanism is still a matter of debate. Besides, the actual

behavior of different types of soil under various rainfall patterns has attracted the interest of researchers. It is the research gaps such as this that provoked this study to be carried out.

# CHAPTER 3

# METHODOLOGY

## 3.1 Introduction

The main objective of this research is to investigate the mechanisms involved in the development of saturation profile. To achieve these objectives, five phases of research activities were undertaken, i.e. research initialization, preliminary preparation, experiments, analysis, and generalization. Figure 3.1 shows the flow chart of the research activities.

The study was initiated by critically reviewing published works related to the topic of rainfall-induced slope failure in order to develop a strong background of the research. The knowledge on the state of the art of the research topic was gained through consultation with several well-known experts such as Professor Harianto Rahardjo from Nanyang Technological University Singapore, Dr. David Toll from University of Durham, Professor Faisal Ali from University of Malaya, Professor Roslan Zainal Abidin from University Technology Mara, and Mr. Law Tien Huat from Mohd. Asby Consultant Sdn. Bhd. Problem statement and hypothesis were formed based on the literature reviews and the professional opinions from experts.

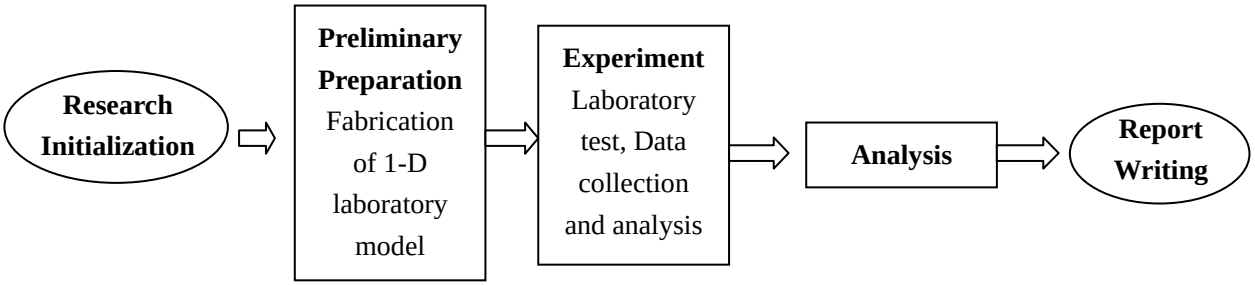


**Figure 3.1** Research framework

The second stage of the research involves the preliminary preparation of experimental apparatus. Numerical analysis was performed to facilitate the preliminary design of the laboratory model.

Investigation on the dominant factors affecting saturation profile and the threshold rainfall patterns for different types of soil were carried out during the third stage of research through numerical simulation. A series of laboratory experiments on a physical soil column model were performed to provide laboratory evidence for the results of numerical simulation.

In the analysis stage, the data obtained from the laboratory tests were analyzed and compared with the results of numerical simulation. Subsequently, discussions were made to explain the dominant factors affecting the saturation profile and its correlation with slope stability.

The last stage of the study was report writing and documentation of research findings.

## 3.2 Setup of Soil Column Model

The soil column model designed for this study consisted of four main parts, i.e.: acrylic soil column, water flow system, instrumentation, and data acquisition system. A three-dimensional diagram of the soil column model is illustrated in Figure 3.2, while the photograph of the apparatus is shown in Figure 3.3.

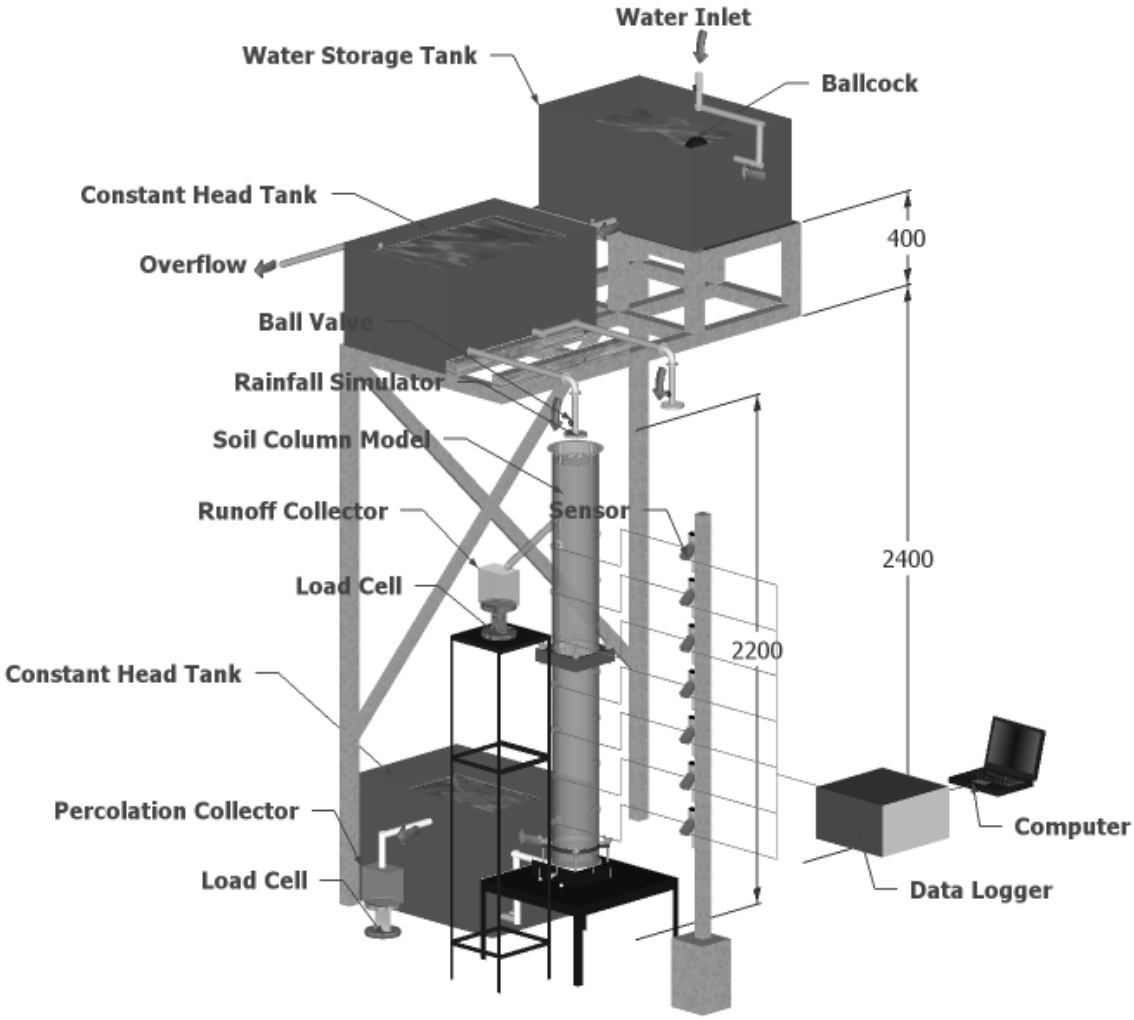


**Figure 3.2** Three-dimensional diagram of the laboratory model setup

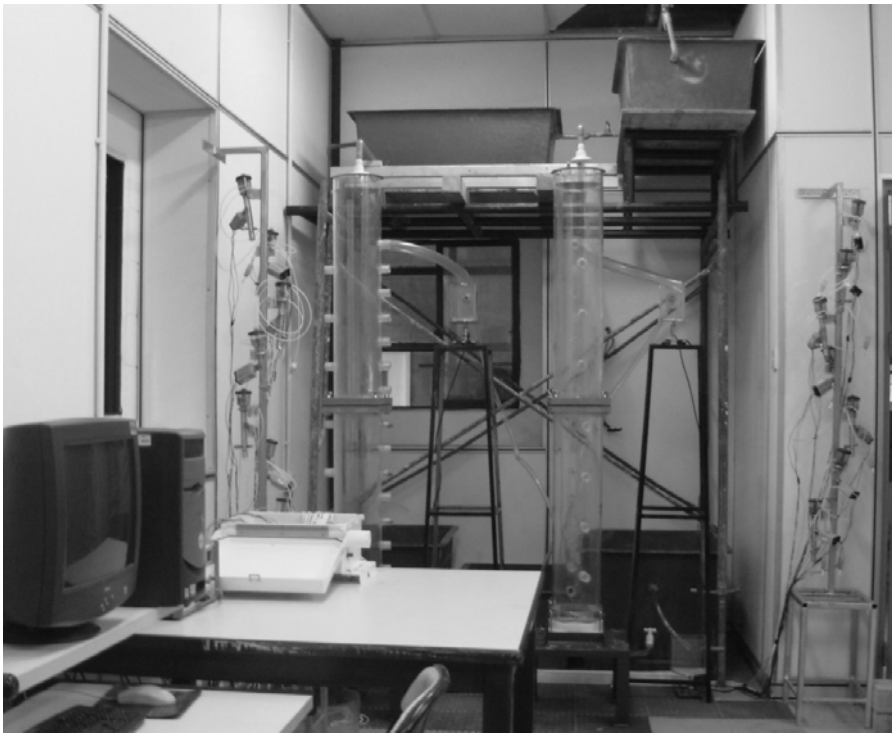

**Figure 3.3** Photograph of the laboratory model setup

### 3.2.1 Soil Column

The soil column was made of acrylic transparent tube with a 5 mm-thick wall and 190-mm internal diameter. The soil column consisted of two separated tubes (900 mm high each) connected securely by clamp system and rubber O- ring. This arrangement was necessary for the ease of compaction and removal of soil sample.

Two types of threaded holes were fabricated on the soil column model wall. One type was used for the installation of tensiometer probes (ceramic cups), while the other was fabricated to install gypsum moisture block. Both threaded holes were spaced at 200 mm along the length of the soil column. The holes that were not in use during an experiment were sealed with threaded plugs.

Screw clamp system was employed to prevent water leakage at the joint between two separated cylinders, and the joint between the cylinder and base plate (Figure 3.4). An O-ring was placed in groove, and fastened with bolts and nuts. The silicon grease was used to improve the resistance to water leakage.

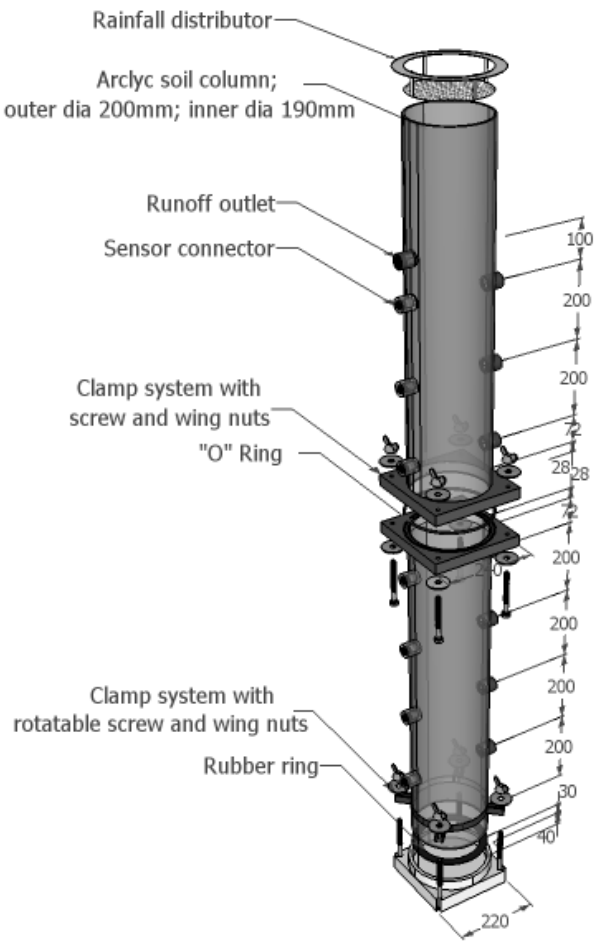


**Figure 3.4** Components of the soil column model

### 3.2.2 Water Flow System

The water flow system of the infiltration column comprises three parts, i.e. inflow/rainfall control, overflow/runoff discharge, and percolation discharge (Figure 3.2)

The inflow/rainfall control consisted of a water storage tank, a constant head tank, a flow regulator (ball valve), and a rainfall distributor. The water storage tank with storage capacity of 216 L was placed 2.8 m from the ground surface. The function of the water storage tank is to provide continuous water flow into the constant head tank. The constant head tank, which was placed immediately below the water storage tank, had a storage capacity of 216L and a constant head of 0.3 m. Water in the storage tank flowed into the constant head tank through a control valve. An overflow outlet was placed at the same level with the inlet flow of constant head tank to create the constant head condition during the test. Beneath the constant head tank was a flow regulator, by which simulated rainfall rate was precisely controlled. Note that this system could only produce flow rate greater than 5mL/min (q = 2.94 ×10-6 m/s).

A perforated aluminum plate was placed on top of the soil column to avoid excessive raindrop energy that may cause erosion on the surface of soils. When a rainfall was applied, the water flowed through the holes of the plate and dripped onto a piece of filter paper that was placed in contact with the surface of the soil column. Through these arrangements, water was delivered to the soil surface in a relatively uniform pattern.

The second component of the water flow system is the overflow / runoff discharge. The overflow discharge system was used to create the no-ponding upper

boundary condition for the soil column. The overflow was discharged as runoff through the outlet located at the soil surface. The runoff was then directed to a load cell that has the capacity of 2 kg, to quantify the runoff rate. Alternatively, the ponding condition can be created by sealing the runoff outlet with a threaded plug.

The last component of the water flow system is the outlet for the discharge of percolated flow. A constant head tank was placed on the floor to maintain the water table at the bottom of the soil column. This was intended to form a clear lower boundary condition. The constant head tank with large open area helped to produce a constant water table with a minimum fluctuation and to allow percolated water in the soil column to drain out freely. The constant head tank was connected to the soil column through a flexible tube. Gravels with the average size of 5mm and a filter paper were placed at the bottom of the soil column to avoid turbulent discharge flow. When water percolated through the soil column, the water flow into the constant head tank and drain out through an overflow outlet placed at the tank. The overflow was directed to a load cell to quantify the rate of percolated flow.

### 3.2.3 Instrumentations

Two types of soil suction measurement instruments were used in the study, i.e. tensiometer and gypsum block. The tensiometer (Soil Moisture Corp. Model 2100F) is equipped with pressure transducer (Soil Moisture Corp. Model 5301-B1). Attempts to measure soil suction higher than 70 kPa during calibration was unsuccessful. Therefore, the gypsum block (Soil Moisture Corp. model 5201F1L06 G-Block) with measurement capacity of 10 kPa to 1500 kPa was introduced. In this study, tensiometer was used to measure soil suction at low range of 0 kPa to 70 kpa (valid for most of the suctions measured in this study), whereas gypsum block was

used to ensure that any suction higher than 70kPa could be traced during the process of setting up initial condition and redistribution. Figure 3.5a and 3.5b show an assembled tensiometer-transducer and gypsum block, respectively.

(a)  (b) 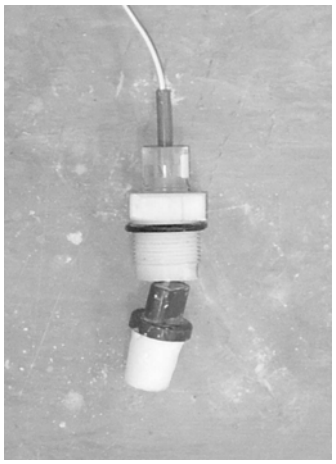

**Figure 3.5** (a) An assembled tensiometer-transducer, (b) Gypsum block

A ceramic cup was installed into the soil column through a predrilled hole after compacting the soil column. The method offers the advantages of protecting the ceramic cup from damage during soil compaction, but care should be taken to ensure that the ceramic cup was closely contacted with the soil particles. To mount the ceramic cup and the tube assembly on the wall of the acrylic column, holes with threaded housing were fabricated on the column wall. A specially designed connector that fit well into the threaded housing, O-ring, and sealing tape were used to form a good seal at the connection. The details of the connector are shown in Figure 3.6.

The connection of gypsum block to soil column consisted of two parts (Figure 3.7). The first part was fitted into the housing, while the second part, facilitated by an “O” Ring, was used to seal the wire fitting to the connector. Since the gypsum block sensor was connected to the data logger via two wires, it was essential to use a wire fitting to provide a cylindrical shape for the ease of sealing. The silicon grout sealer was injected into the space in between the wire fitting and

wires to provide a good seal.

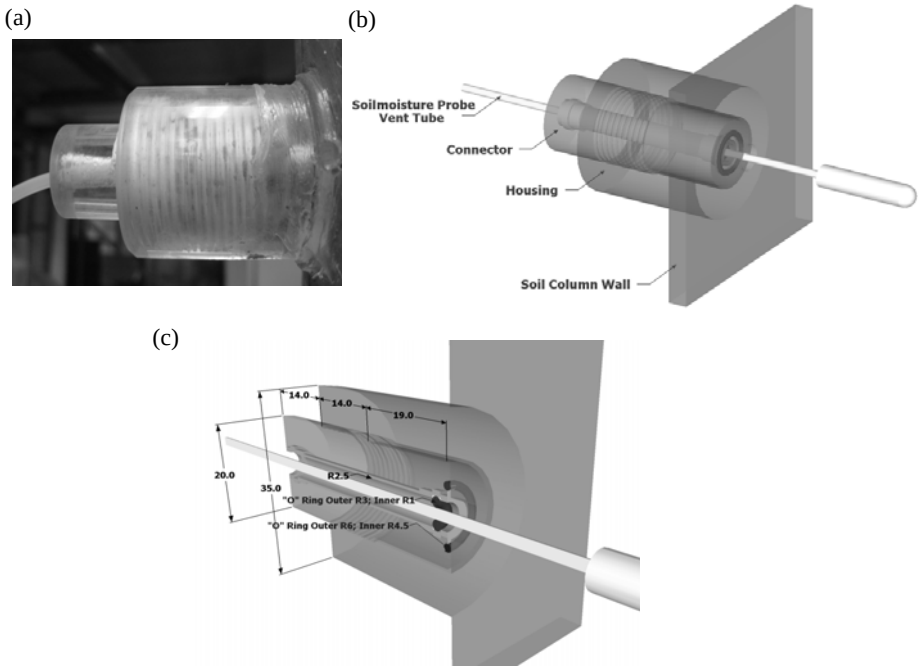


**Figure 3.6** (a) Photograph, (b) Three-dimensional diagram, and (c) Cross-sectional view of the tensiometer connector

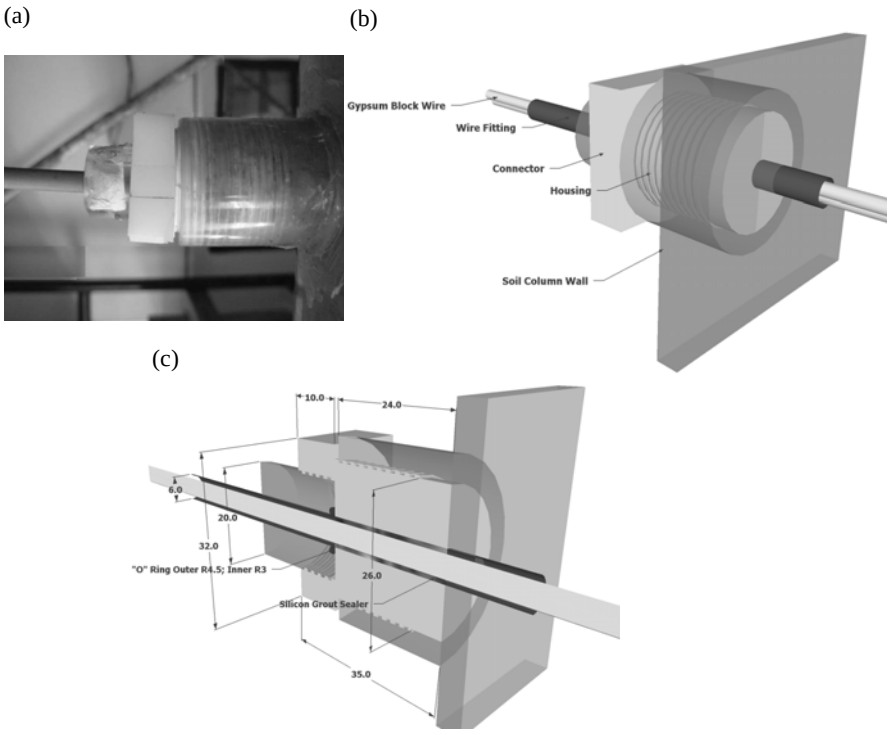


**Figure 3.7** (a) Photograph, (b) Three-dimensional diagram, and (c) Cross-sectional view of the gypsum block

### 3.2.4 Data Acquisition System

The data acquisition system used in the study comprises two units of data logger, a solid state relay, an external power supply, and a personal computer, as shown in Figure 3.8. The tensiometers and gypsum blocks were connected to the Campbell Scientific Data Logger, model CR10x (Campbell Scientific Inc.), while the load cells were connected to the GDS 8 Channel Serial Data Acquisition Pad.

The CR10x data logger consisted of two units of 32 single-ended channels multiplexer (model MUX AM416). A program was written to set up communication and data collection between the data logger and instruments, as presented in Appendix A. Besides, a controlling software named PC208W version 2.3 was used to execute the data logger.

The CR10x data logger was powered up by an internal 12 V battery but the optimum power requirement for the tensiometer transducer system was 24 V. Therefore, the tensiometer transducer system was connected to an external 24 V power supply via a solid state relay. The functions of the solid state relay are to protect the data logger circuit and to switch on the power only when the triggering signal from data logger was received. These functions are essential to protect the tensiometer transducer system from over-heated due to long operating durations.

The GDS 8 Channel Serial Data Acquisition Pad is a data logger with eight channels of 16-bit data acquisition. The configuration of the data logger was originally designed to log the data for shearing machine. Some modifications have been made to allow the logging of four load cells concurrently. A controlling software named GDSLAB v2 was used to communicate with the GDS data logger.

The data from the data logger units were transferred to the personal computer periodically through the serial ports. The data stored in the personal computer were normally set in a format of pressure versus real time at a desired interval. An interval of 15-min was used in this study.

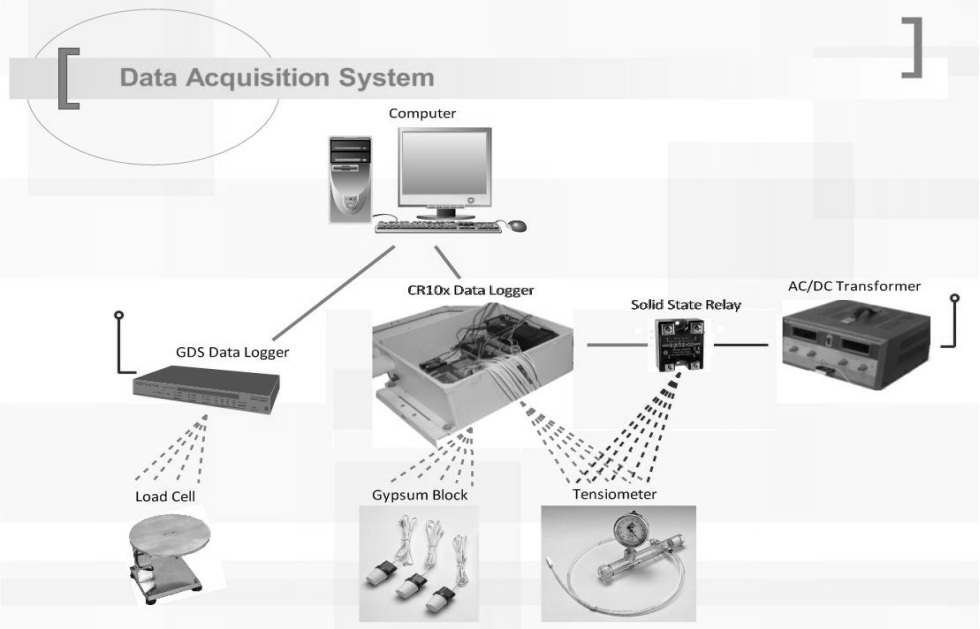


**Figure 3.8** Data acquisition system

# CHAPTER 4

# DATA AND DISCUSSIONS

## 4.1 Introduction

This chapter presents the results of one-dimensional infiltration tests carried out in the laboratory. A total of ten tests were carried out for different combinations of rainfall patterns and soil types.

## 4.2 Soil Materials

Four types of soil were employed in the study, i.e. sand-gravel, silty gravel, sandy silt, and silt (kaolin). These soil types were chosen to simulate a maximum, a minimum, and the intermediate conditions with respect to the hydraulic properties and particle sizes of soils. A series of laboratory tests were conducted to determine the soil properties. Figure 4.1, 4.2, 4.3, and 4.4 shows the particle size distribution (PSD), soil water characteristic curve (SWCC), hydraulic conductivity functions and scanning electron micrograph (SEM) images of the soils, respectively. The physical properties of the soils are tabulated in Table 4.1.

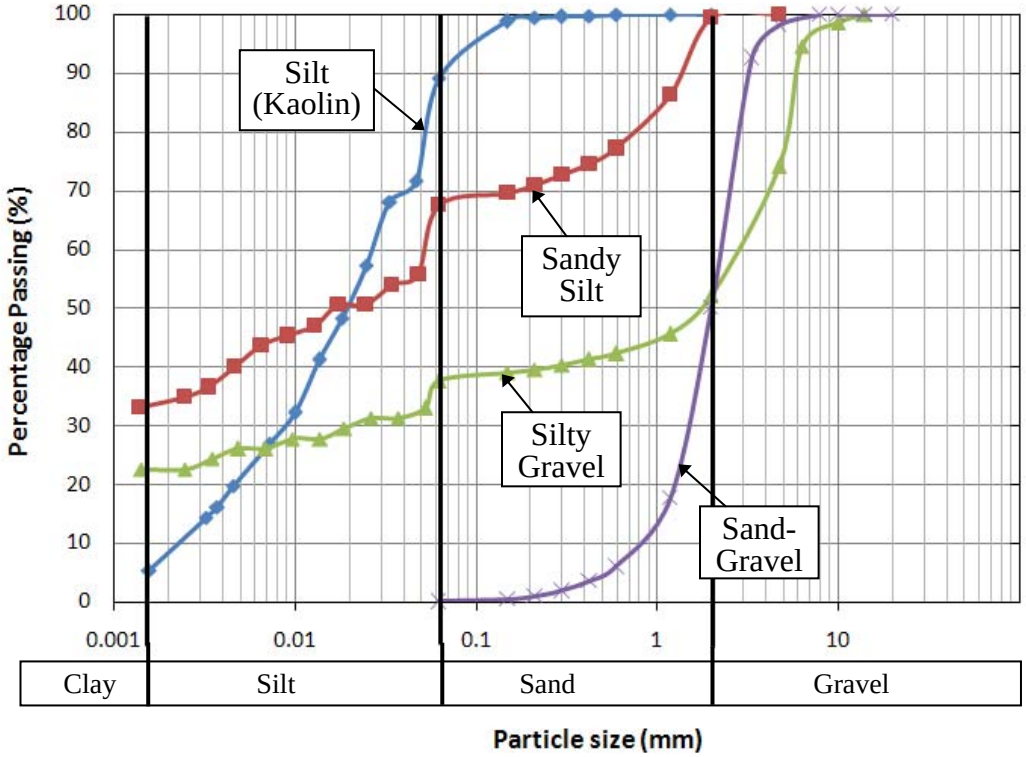


**Figure 4.1** Particle size distributions of the soils

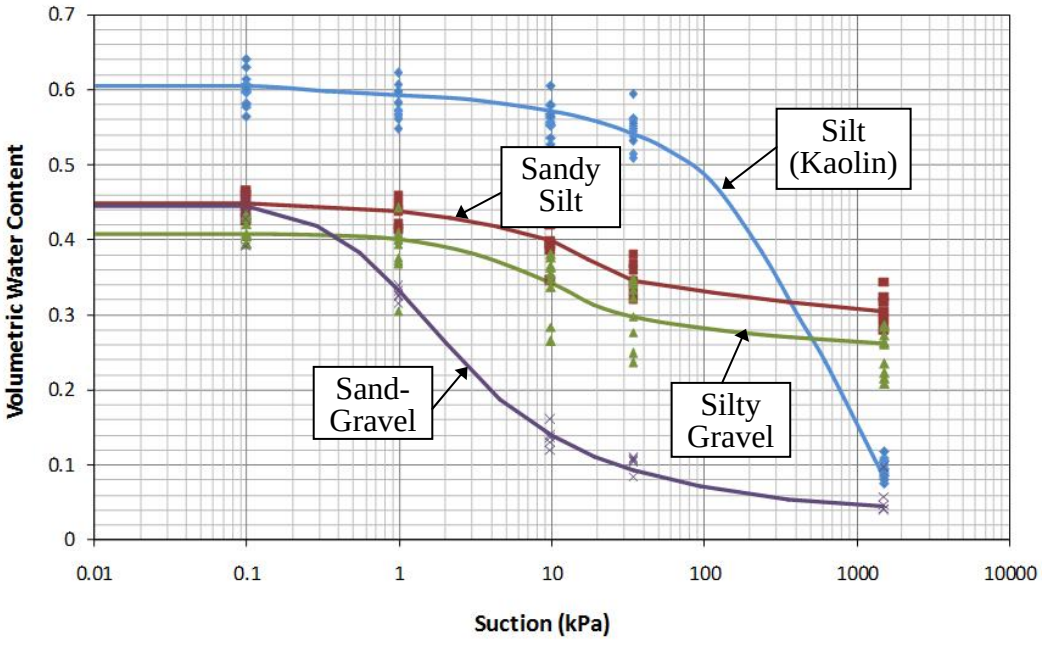


**Figure 4.2** SWCC of the soils

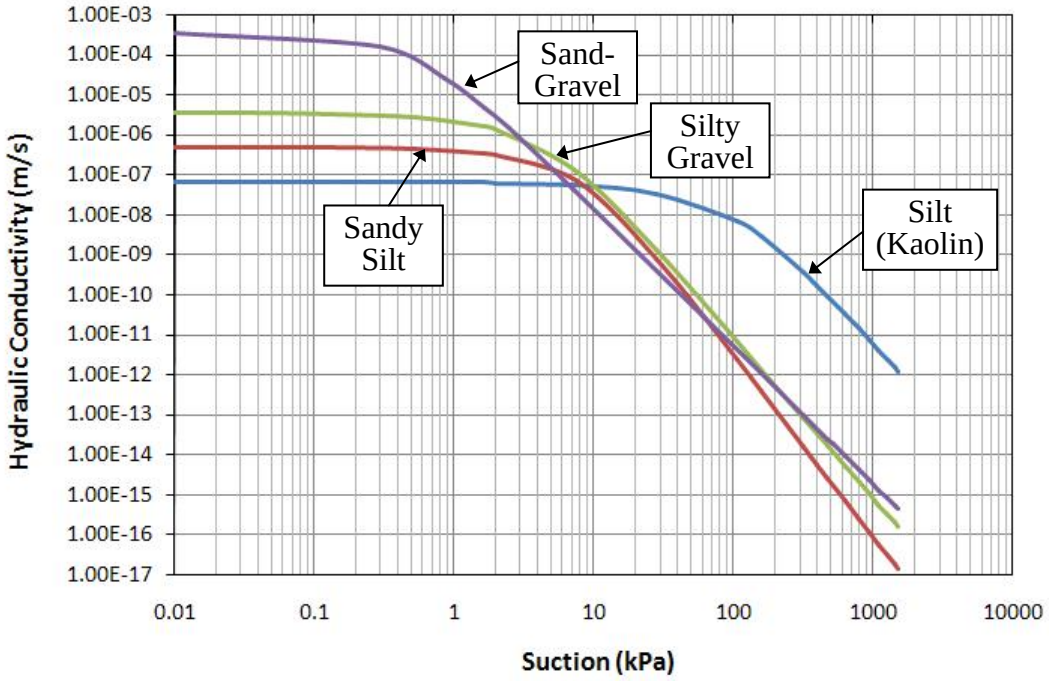


**Figure 4.3** Hydraulic conductivity function of the soils

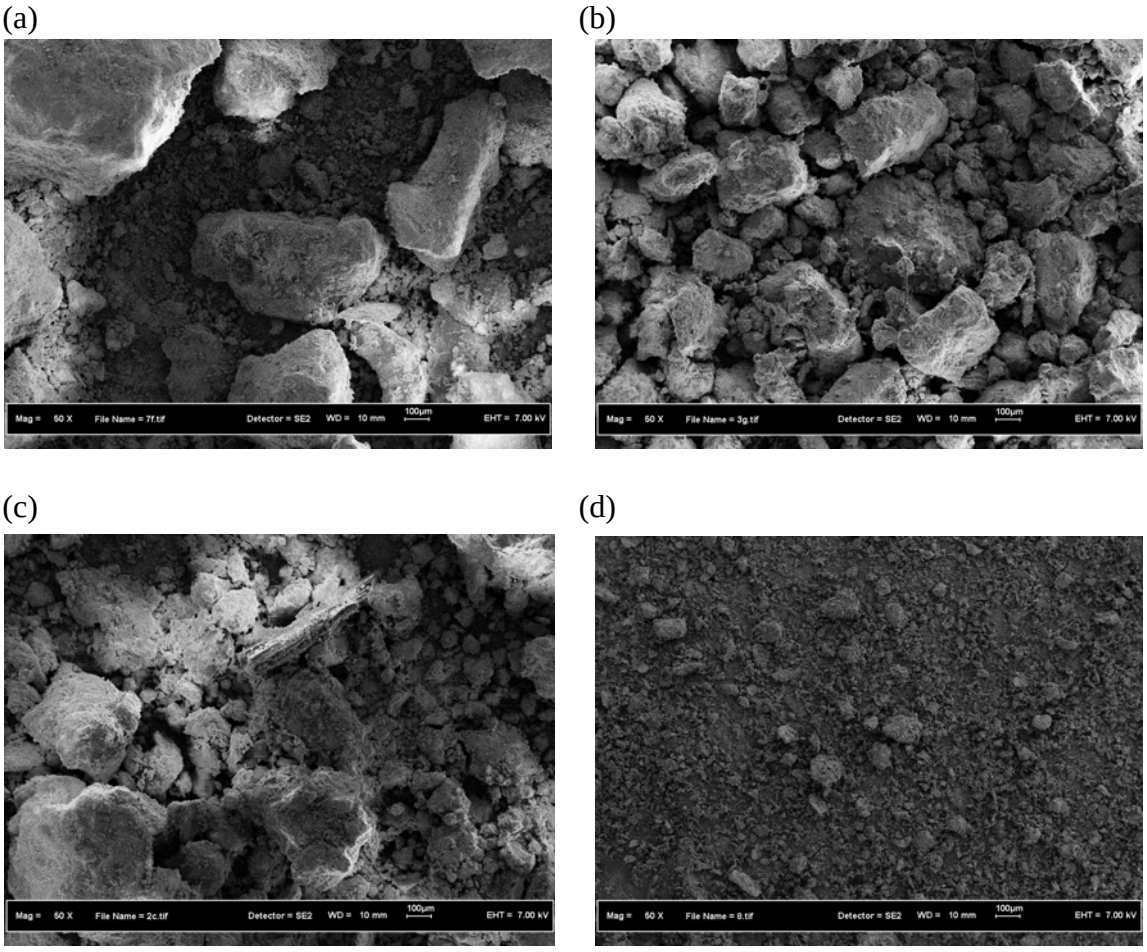


**Figure 4.4** SEM images of (a) sand-gravel, (b) silty gravel, (c) sandy silt, and (d) silt (kaolin)

**Table 4.1:** Physical properties of the soils

| | **Sand-Gravel** | **Silty Gravel** | **Sandy Silt** | **Silt (Kaolin)** |
|---|---|---|---|---|
| **Composition** | | | | |
| Gravel (%) | 50 | 48 | 0 | 0 |
| Sand (%) | 50 | 15 | 33 | 11 |
| Silt (%) | 0 | 20 | 34 | 81 |
| Clay (%) | 0 | 17 | 33 | 8 |
| **LL (%)** | - | 53.2 | 59.3 | 44.8 |
| **PL (%)** | - | 35.5 | 31.9 | 30.6 |
| **PI** | - | 17.7 | 27.4 | 14.2 |
| **Soil Classification BSCS** | S-GP | GMH | MHS | MI |
| **$G_s$** | 2.65 | 2.65 | 2.63 | 2.52 |
| **$\rho_b$ (kg/m$^3$)** | - | 1805 | - | - |
| **$\rho_d$ (kg/m$^3$)** | - | 1366 | - | - |
| **MDD (kg/m$^3$)** | - | - | 1415 | 1587 |
| **OMC (%)** | - | - | 31.0 | 19.3 |
| **Density @ $e_{max}$ (kg/m$^3$)** | 1856 | - | - | - |
| **$K_{sat}$ (m/s)** | $3.44 \times 10^{-4}$ | $3.68 \times 10^{-6}$ | $5.00 \times 10^{-7}$ | $6.78 \times 10^{-8}$ |
| **CU Test** | | | | |
| c' (kPa) | - | - | 7.6 | 9.2 |
| $\phi'(^o)$ | - | - | 32.1 | 17.6 |
| **Direct Shear** | | | | |
| c' (kPa) | 1.2 | 3.3 | - | - |
| $\phi'$ ($^o$) | 38.7 | 39.5 | - | - |

## 4.3 Experimental Design

Table 4.2 summarizes the description of infiltration test performed in this study. The initial conditions for sand, silty gravel and sandy silt were set at residual volumetric water content, while the initial condition for kaolin was simulated from the field measurement (Gofar *et al.*, 2007). These initial conditions were created by mixing the dry soil with the corresponding volumetric water content during the compaction. Note that the ponding condition for tests no. 7 and 10 were created by maintaining a water level of 10 mm above the soil surface.

**Table 4.2:** Experimental design for infiltration tests

| Test | Soil Type | Rainfall duration (hour) | Rainfall intensity (m/s) | Top Boundary Condition | Remark |
|---|---|---|---|---|---|
| 1 | Sand-Gravel | 1 | $1.84 \times 10^{-5}$ | $q < k_{sat}$ | |
| 2 | Sand-Gravel | 24 | $3.35 \times 10^{-6}$ | $q < k_{sat}$ | |
| 3 | Silty Gravel | 1 | $1.84 \times 10^{-5}$ | $q > k_{sat}$ | Runoff |
| 4 | Silty Gravel | 24 | $3.35 \times 10^{-6}$ | $q < k_{sat}$ | Runoff |
| 5 | Sandy Silt | 1 | $1.84 \times 10^{-5}$ | $q > k_{sat}$ | Runoff |
| 6 | Sandy Silt | 24 | $3.35 \times 10^{-6}$ | $q > k_{sat}$ | Runoff |
| 7 | Sandy Silt | 120 | - | Ponding | |
| 8 | Silt (Kaolin) | 1 | $1.84 \times 10^{-5}$ | $q > k_{sat}$ | Runoff |
| 9 | Silt (Kaolin) | 24 | $3.35 \times 10^{-6}$ | $q > k_{sat}$ | Runoff |
| 10 | Silt (Kaolin) | 120 | - | Ponding | |

Figure 4.5 (a-d) shows the setup of the soil column models for the four types of soil. From the laboratory measurements, the initial suction for sand-gravel (approximately 8 kPa) was slightly lower than that of estimated from the SWCC (10 kPa). The differences were probably caused by the inefficiency in the tensiometer to measure the suction in granular soil since the contact between ceramic sensor and

soil particles were poor. For the silty gravel, sandy silt and silt (kaolin) which contained considerable amount of cohesive particles, the contact between ceramic sensor and soil particles were significantly improved, hence the suction measurements showed good agreement with the value predicted from SWCC. The measured initial suctions for silty gravel, sandy silt and silt (kaolin) were 17 to 23 kPa, 26 to 32 kPa, and 46 to 50 kPa, respectively.

(a) (b)

(c) (d)

**Figure 4.5** The setup of soil column models for (a) sand-gravel, (b) silty gravel, (c) sandy silt, and (d) silt (kaolin)

## 4.4 Relationships between Infiltration and Runoff

Figure 4.6 (a-c) illustrates the relationships between infiltration and runoff for silty gravel, sandy silt and silt (kaolin). It should be noted that the runoff was not generated throughout the experiments of sand-gravel column. This was because the applied rainfall has an intensity lower than the saturated permeability of soil.

(a)

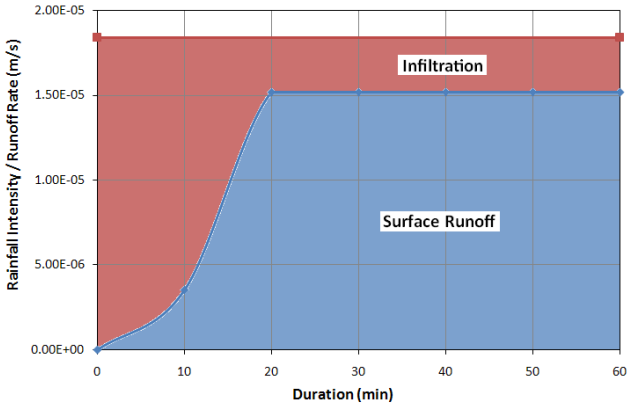


(b)

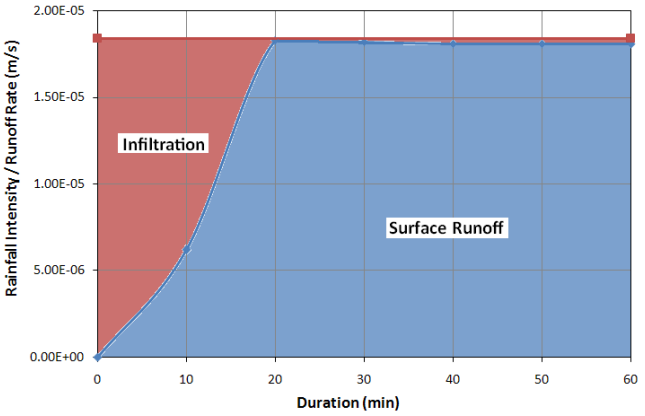


(c)

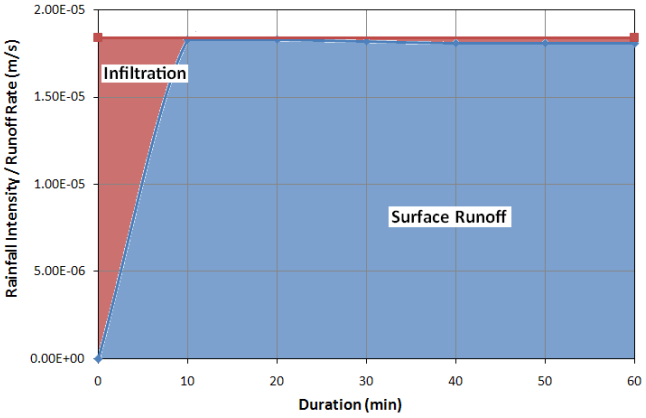


**Figure 4.6** Relationships between rainfall and surface runoff for (a) silty gravel, (b) sandy silt, and (c) silt (kaolin)

As shown in Figure 4.6a, the rainfall infiltrated effectively into the silty gravel for the first 10 minutes. Subsequently, the surface runoff was generated and the rate of infiltration and runoff became constant after 20 minutes. The measured runoff rate was $1.52 \times 10^{-5}$ m/s indicating large portion of rainfall has contributed to the surface runoff (the applied rainfall = $1.84 \times 10^{-5}$ m/s). Subtracting the surface runoff from the applied rainfall, the effective infiltration rate was $3.2 \times 10^{-6}$ m/s. This value was very close to the saturated permeability of silty gravel ($k_{sat} = 3.68 \times 10^{-6}$ m/s).

The amount of surface runoff was greater for the soils with lower saturated permeability. For instances, the runoff rate of sandy silt ($k_{sat} = 5.00 \times 10^{-7}$ m/s) constant at $1.81 \times 10^{-5}$ m/s, indicating the infiltration rate was $3.0 \times 10^{-7}$ m/s. As for the silt ($k_{sat} = 6.78 \times 10^{-8}$ m/s), the runoff rate constant at $1.83 \times 10^{-5}$ m/s with the infiltration rate approximated to $1.0 \times 10^{-7}$ m/s. This infiltration rate, however, was almost twice the magnitude of saturated permeability of silt (kaolin) obtained from the falling head permeability test. It was thought that the tendencies of silt (kaolin) to shrink and crack have caused the infiltration capacities far in exceedance of the expected saturated permeability. This finding was supported by the observation of the desiccated surface and cracks at the silt (kaolin) column. (Figure 4.7).

**Figure 4.7** Cracks formed at the surface of silt (kaolin)

## 4.5 Saturation Profiles

The saturation profiles for the prescribed test combinations were measured as shown in Figure 4.8. In the sand-gravel column (Figure 4.8a), the short and intense 1-hour major rainfall has resulted in the lowest minimum suction value, but limited to a very shallow depth of 0.3 m. Conversely, the wetting front resulted from the long and less intense 24-hour major rainfall has advanced beyond the entire length of the soil column (1.5m). This was revealed through the measurement of percolated flow at the bottom of the soil column after eight hours of rainfall. Whilst the wetting front was much deeper, the minimum suction value induced by the 24-hour major rainfall was just slightly higher than that of 1-hour major rainfall.

The silty gravel column exhibited similar trend as the sand-gravel (Figure 4.8b). It should be noted that the intensity of 1-hour rainfall ($1.84 \times 10^{-5}$ m/s) was greater than the saturated permeability of silty gravel ($k_{sat} = 3.68 \times 10^{-6}$ m/s). Under such circumstances, the effective infiltration of silty gravel was controlled by the saturated permeability, hence the minimum suction value induced by the 1-hour rainfall was almost identical to that of 24-hour rainfall ($i = 3.35 \times 10^{-6}$ m/s). Nonetheless, the 24-hour rainfall still resulted in deeper wetting front than the 1-hour rainfall. The results implied that for $q/k_{sat} < 1$, the minimum suction value is governed by the rainfall intensity, while the wetting front depth was influenced by the total amount of rainfall infiltrated into the soil. As for $q/k_{sat} > 1$, the infiltration and minimum suction value was controlled by the saturated permeability, while the wetting front depth was only influenced by the rainfall duration.

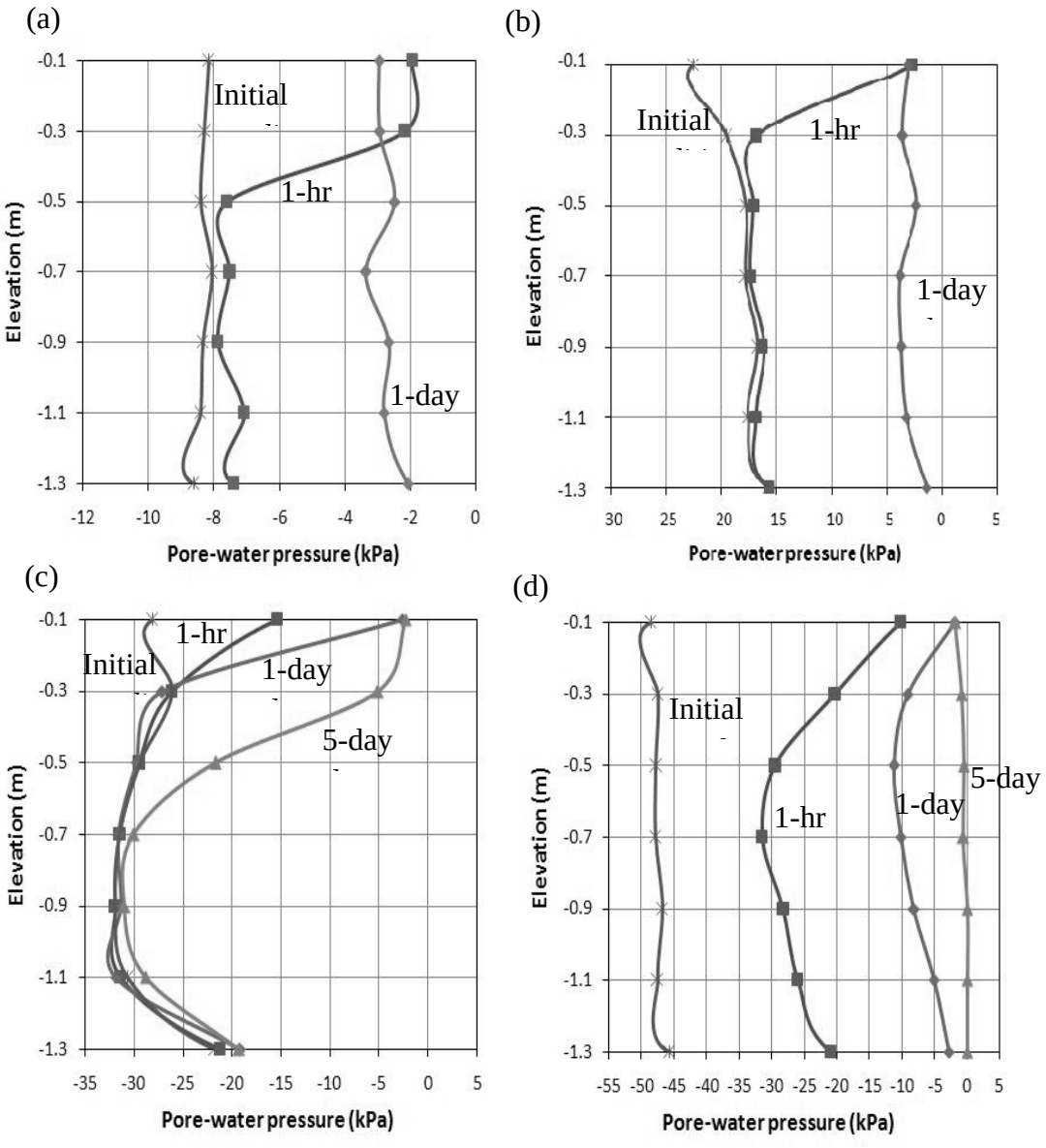


**Figure 4.8** Saturation profiles in (a) sand-gravel, (b) silty gravel, (c) sandy silt, and (d) silt (kaolin)

The wetting front measured in the laboratory was only 0.3 m. The inhomogeneity in the compacted soils, and the inconsistency between the measured and actual SWCC as well as the predicted hydraulic conductivity function could be the reason for these deviations.

In addition to the 1-hour and 24-hour major rainfalls, a ponding condition was created in the sandy silt column to study the response of suction distribution to the infiltration of longer duration (5 days). Whilst the minimum suction value was the same as the 24-hour major rainfall, the 5-day infiltration has resulted in a deeper wetting front.

The mechanism of suction loss in sandy silt under rainfall infiltration condition is as follows: (1) the low saturated permeability of sandy silt limits the infiltrated rainfall amount, hence large amount of rainfall contributes to runoff, (2) the infiltrated rainfall reduces the soil suction gradually until a minimum suction value is achieved, (3) beyond this point, the rainfall infiltration will cause deeper propagation of wetting front. Apparently, the long duration rainfall appears to be a more critical rainfall for sandy silt.

For the silt (kaolin) column, the suction distribution measured in the laboratory was generally lower than that of numerical prediction (Figure 4.8d). The results indicated that more water was actually infiltrating into the soil due to the cracks and desiccated surfaces. Besides, the capillary rise effect was found very significant in kaolin. The upward flow from the simulated water table has caused the suction loss at the bottom of the soil column.

In conclusion, the initial suction of coarse-grained soil is lower than fine-grained soil. In fact, the suctions of 2 to 4 kPa were very common for sand-gravel soil under typical rainfall condition. While the initial suction of fine-grained soil was higher, the capillary rise effect from the water table was comparatively significant. It is thus essential to consider the effect of water table on the suction distribution of fine-grained soil slope if the water table is high.

## 4.6 Suction Redistributions

The redistribution pattern for each laboratory test was observed until the initial suction condition was obtained. Figure 4.9 (a-d) illustrates the redistribution pattern after the 24-hour rainfall for sand-gravel, silty gravel, sandy silt and silt (kaolin), respectively.

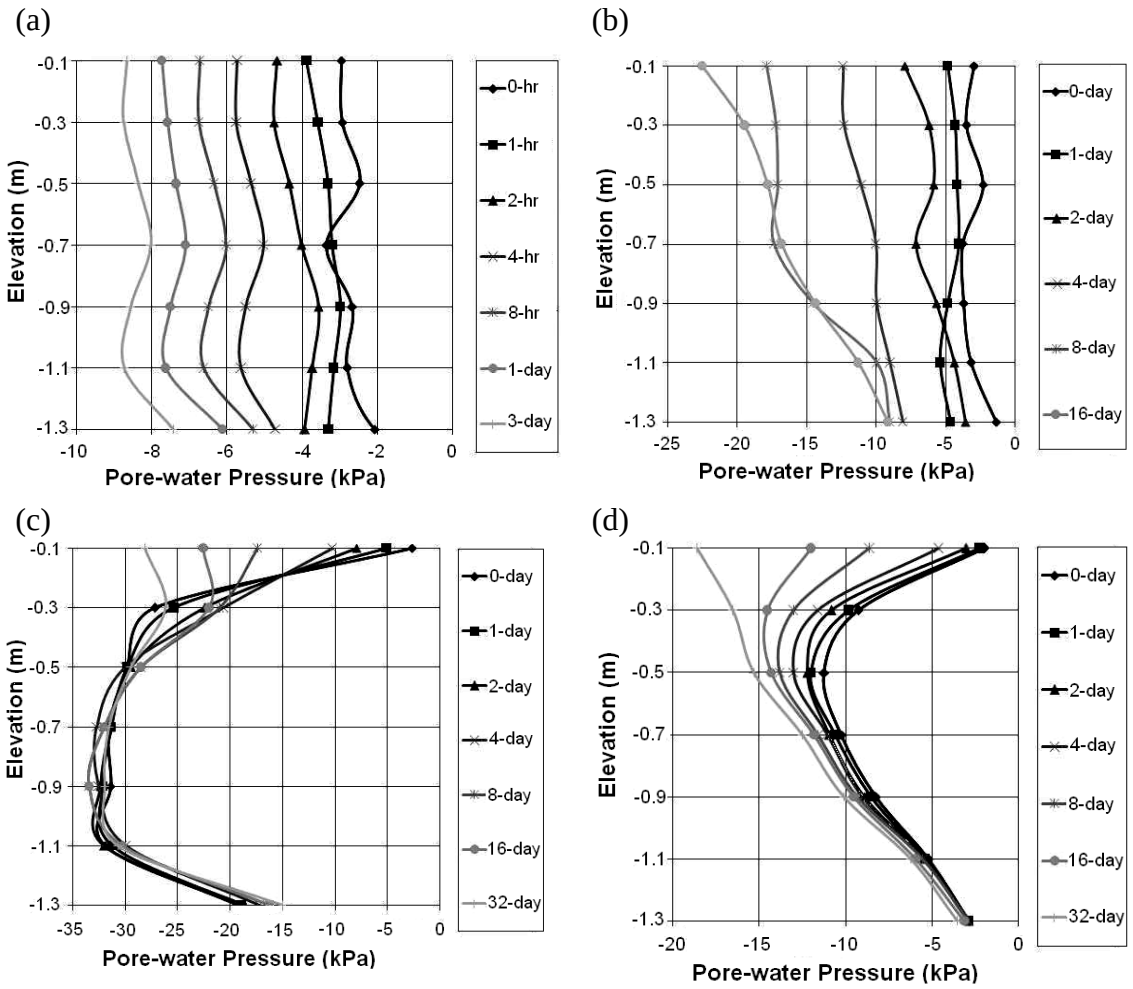


**Figure 4.9** Suction redistributions in (a) sand-gravel, (b) silty gravel, (c) sandy silt, and (d) silt (kaolin)

In general, the water content in coarse-grained soil redistributed quicker than that of fine-grained soil. Three days was required for the sand-gravel to regain its

initial condition after the 24-hour rainfall event. However, 16 days and 32 days were required for silty gravel and sandy silt, respectively. As for silt (kaolin), the initial condition was not recovered after 32 days of drying. The phenomena can be explained by the low saturated permeability of fine-grained soil. However, as observed in the SWCC and hydraulic conductivity function (refer to Figure 4.2 and 4.3), the permeability of coarse-grained soil decreased in tandem with the increase of suction, until a stage where the permeability of coarse-grained soil could be lower than that of fine-grained soil. This behaviour of soil has caused the redistribution rate of coarse-grained soil decrease in exponential fashion towards the higher suction. As for the fine-grained soil (i.e. silt), the redistribution rate was more consistent over the suction range concerned.

## 4.7 Concluding Remarks

In the laboratory soil column tests, the behaviours of four types of soil (i.e. sand, silty gravel, sandy silt and kaolin) under various rainfall conditions were investigated. In general, the responses of suction distribution and redistribution to the rainfall infiltration were governed by the SWCC and hydraulic conductivity of soil.

The suction existed in the soil with high saturated permeability (i.e. sand) was very low (typically in between 2 to 4 kPa). The short and intense major rainfall (i.e. 1-hour rainfall) has resulted in the lowest minimum suction value, but limited to a very shallow depth (i.e. 0.3 m)

For soil with moderate saturated permeability (i.e. silty gravel and sandy silt), both major rainfall and antecedent rainfall could govern the suction distribution.

The initial suctions existed in these types of soil were relatively high (18 to 33 kPa). However, the redistribution rate was significantly reduced by the existence of the fine particles.

For soil with low saturated permeability (i.e. silt), the suction distribution was more influenced by the duration of rainfall. The longer the duration of rainfall, the lower the suction generated. At the initial condition, the suction in silt (kaolin) can be as high as 50kPa. However, the suction decreased gradually when the soil column was subjected to rainfall infiltration. The lowest suction measured in the laboratory test was 0kPa, indicating $q/k_{sat} > 1$. Despite of the fact that the infiltration was limited by the soil's saturated permeability, the suction can be altered significantly with little changes in the water content. Besides, the shrink and crack behaviours of clayey soil permitted more water to infiltrate into the soil through the desiccated surface.

In general, the water content in the coarse-grained soil redistributed quicker than the fine-grained soil. The initial suctions were regained in sand-gravel, silty gravel and sandy silt after 3 day, 16 days, and 32 days, respectively. However, the initial condition of 50 kPa in silt (kaolin) was not recovered after 32 days of drying. The slow redistribution rate can be attributed to the high water retention ability and low saturated permeability of fine-grained soil.

# CHAPTER 5

# CONCLUSIONS AND SUGGESTIONS

## 5.1 Introduction

A study on the saturation profile for various combinations of rainfall pattern and soil type is reported in this thesis. The specific objectives of the study were stated in the Chapter 1, as the ultimate goal of the study is to investigate the mechanisms involved in the development of saturation profile. In this Chapter, the conclusions of the study are presented after which the recommendations for further research are presented.

## 5.2 Conclusions

The main outcomes and conclusions of the study are drawn in view of the objectives as formulated on page 2.

### 5.2.1 Laboratory Model for Saturation Profile Study

A soil column model was fabricated to study the saturation profile in four types of soil under various rainfall conditions. The model was found to be function properly to quantify the rainfall intensity, surface runoff rate, pore-water pressure, and percolated flow rate.

### 5.2.2 Dominant Factors Affecting Saturation Profile

The rainfall patterns and soil properties are two important parameters affecting the saturation profile developed in the soil. Generally, the coarse-grained soil is characterized by high permeability and low water retention ability. As such, the suction existed in the coarse-grained soil is generally low, typically within 2 to 4kPa. Under these circumstances, the effect of rainfall pattern on the saturation profile of coarse-grained soil is relatively insignificant compared to fine-grained soil.

Conversely, the fine-grained soil is characterized by low permeability and high water retention ability. Whilst the response of suction variation to the rainfall infiltration is considerably slow, the variation of suction can be very significant due to the wide differences of suction between dry condition and wet condition. The prolonged rainfall could induce greater changes in saturation profile of this type of soil. The shrink and crack nature of the fine-grained soil has not helped the problem but allow more water to infiltrate into the surficial soil through the desiccated surface.

### 5.2.3 Development of Saturation Profile

The mechanism of the development of saturation profile in soil can be explained as follows: (1) the saturated permeability of soil controls the infiltrated rainfall amount if the rainfall intensity is higher than the soil's permeability, (2) the infiltrated rainfall retains near the soil surface and saturate the soil gradually until a minimum suction value is achieved, (3) beyond this point, the rainfall infiltration will cause deeper propagation of wetting front. Apparently, the longer rainfall duration would cause deeper wetting front in soil. In general, the saturation profile observed in the laboratory model showed good agreement with the results from numerical simulation. Nonetheless, the accuracy of the numerical predictions is governed by the consistency of the soil properties input parameters e.g. SWCC and hydraulic conductivity between numerical simulation and actual soil behaviour.

## 5.3 Suggestions for Future Researches

In light of the limitations of the present study, a few areas were identified where further research were required:

i. **The study on a full scale model constructed under natural environment.** From the field measurement, it was found that the changes in ambient environment (i.e. solar radiation, humidity, temperature etc.) could also alter the soil suction. It would enhance the findings from the present study by accounting more surface boundary conditions.

ii. **The numerical simulation and laboratory modeling by using two dimensional slope model.** The two dimensional analysis is required to consider for the horizontal flow in the soil slope.

iii. **The study on the behaviour of layered soil.** The behaviour of homogeneous soil has been investigated in the present study. It is believed that the findings from the present study could provide the fundamental knowledge for the study in the behaviour of layered soil which sustained much more complexity.

iv. **The improvement on the laboratory modeling technique, particularly for the rainfall simulator.** An advanced rainfall simulator should be used to enable the simulation of low rainfall intensity for longer duration of antecedent rainfall. Besides, the installation of Time-Domain Reflectometry (TDR) probe that provides the measurement of volumetric water content would allow the inferences of the suction measurements from tensiometer.

v. **The study on the mitigation measures of rainfall-induced slope failure.** The mechanisms of the rainfall-induced slope failure for different types of soil have been identified in this study. The further study may look into the possible mitigation measures.

## REFERENCES

Agus, S.S., Leong, E.C. and Rahardjo, H. (2001). Soil-Water Characteristic Curves of Singapore Residual Soils. *Journal of Geotechnical and Geological Engineering*. 19: 285-309.

Bao, C.G., Gong, B. and Zhan, L. (1998). Properties of Unsaturated Soils and Slope Stability of Expansive Soil. Keynote Lecture, *2nd Int. Conf. on Unsaturated Soils*. Beijing, China.

Bouwer, H. (1966). Rapid Field Measurement of Air Entry Value and Hydraulic Conductivity of Soil as Significant Parameters in Flow System Analysis. *Water Resources Research*. 2(4): 729-738.

Brisson, P., Garga, V.K. and Vanapalli, S.K. (2002) Determination of Unsaturated Flow Characteristics of Nickel Mine Tailings. *55th Canadian Geotechnical Conference*, Niagara, Canada, October 2002.

Cai, F. and Ugai, K. (2004). Numerical Analysis of Rainfall Effects on Slope Stability. *International Journal of Geomechanics, ASCE.* 4(2): 69-78.

Fredlund, D.G. and Rahardjo, H. (1993). *Soil Mechanics for Unsaturated Soils*. New York: John Wiley & Sons, Inc.

Fredlund, D. G. and Xing, A. (1994). Equations for the Soil-Water Characteristic Curve. *Canadian Geotechical Journal*. 31: 521–532.

Fredlund, D.G., Xing, A. and Huang, S. (1994). Predicting the Permeability Function for Unsaturated Soils Using the Soil-Water Character Curve. *Canadian Geotechnical Journal*. 31(3): 533-546

Freeze, R. A. and Cherry, J. A. (1979). *Groundwater*. New York: Prentice-Hall, Inc.

Gasmo, J. M., Rahardjo, H., and Leong, E. C. (2000). Infiltration Effects on Stability of a Residual Soil Slope. *Computer Geotechnique.* 26: 145–165.

Geiger, S.L., and Durnford, D.S. (2000). Infiltration in Homogeneous Sands and a Mechanistic Model of Unstable Flow. *Soil Science Society of America Journal*. 64: 460-469.

GEO-SLOPE International Ltd. (2004). *Seepage Modeling with SEEP/W*. Calgary, Alta., Canada.

Gitirana, G.Jr. and Fredlund, D.G. (2004). Soil-Water Characteristic Curve Equation with Independent Properties. *Journal of Geotechnical and Geoenvironmental Engineering, ASCE*. 130(2): 209-212.

Glass, R.J., Steenhuis, T.S., and Parlange, J.Y. (1989). Wetting Front Instability, Experimental Determination of Relationships between System Parameters and Two Dimensional Unstable Flow Field Behavior in Initially Dry Porous Media. *Water Resource Research*. 25: 1195-1207.

Gofar, N., Lee, M.L. and Kassim, A. (2007) Stability of Unsaturated Slopes Subjected to Rainfall Infiltration. *Proceedings of the Fourth International Conference on Disaster Prevention and Rehabilitation*, Semarang 10-11 September 2007: 158-167.

Green, W.H. and Ampt, G.A.. (1911). Studies on Soil Physics I. The Flow of Air and Water through Soils. *Journal of Agricultural Research*. 4: 1-24.

Gribb, M.M., Kodesova, R. and Ordway, S.E. (2004). Comparison of Soil Hydraulic Property Measurement Methods. *Journal of Geotechnical and Geoenvironmental Engineering, ASCE*. 130(10): 1084-1095.

Horton, R.E. (1933). The role of infiltration in the hydrological cycle. *Trans. American Geophys. Union*. 14: 446-460.

Joel, A., Messing, I., Seguel, O., and Casanova, M. (2002). Measurement of surface water runoff from plots of two different sizes. *Hydrological Processes*. 16(7): 1467-1478.

Kim, J., Park, S. and Jeong, S. (2006). Effect of Wetting Front Suction Loss on Stability of Unsaturated Soil Slopes. *Unsaturated Soils, Seepage, and Environmental Geotechnics, ASCE*. 148: 70-77.

Leong, E.C. and Rahardjo, H. (1997). Permeability Functions for Unsaturated Soils. *Journal of Geotechnical and Geoenvironmental Engineering, ASCE*. 123(12): 1118-1126.

Li, A.G., Tham, L.G., Yue, G.Q., Lee, C.F. and Law, K.T. (2005). Comparison of Field and Laboratory Soil-Water Characteristic Curves. *Journal of Geotechnical and Geoenvironmental Engineering, ASCE*. 131(9): 1176-1180.

Liu, Y., Bierck, B.R., Selker, J.S., Steenhuis, T.S. and Parlange, J.Y. (1993). High Density X-Ray and Tensiometer Measurements in Rapidly Changing Preferential Flow Fields. *Soil Science Society of America Journal*. 57: 1188-1192.

Loáiciga, H.A. and Huang, A. (2007). Ponding Analysis with Green-and-Ampt Infiltration. *Journal of Hydrologic Engineering, ASCE*. 12(1): 109-112.

Lumb, P. B. (1962). The Properties of Decomposed Granite: *Geo- technique*. 12: 226-243.

Lumb, P. B. (1975) Slope Failures in Hong Kong. *Journal of Engineering Geology.* 8: 31–65.

Mein, R.G. and Farrell, D.A. (1974). Determination of Wetting front Suction in the Green-Ampt Equation. *Soil Science Society of America, Proceeding*. 38: 872-876.

Mein, R.G. and Larson, C.L. (1973). Modeling Infiltration during a Steady Rain. *Water Resources Research*. 9(2): 384-394.

Neuman, S.P. (1976). Wetting Front Pressure Head in the Infiltration Model of Green and Ampt. *Water Resources Research*. 12(3): 564-566.

Ng, C.W.W., Zhan, L.T., Bao, C.G., Fredlund, D.G., and Gong, B.W. (2003). Performance of Unsaturated Expansive Soil Slope Subjected to Artificial Rainfall Infiltration. *Géotechnique*. 53(2): 143–157.

Pradel, D. and Raad, G. (1993). Effect of Permeability on Surficial Stability of Homogeneous Slopes. *Journal of Geotechnical Engineering, ASCE*. 119(2): 315-332.

Sung, E.C. and Seung, R.L. (2002). Evaluation of Surficial Stability for Homogeneous Slopes Considering Rainfall Characteristics. *Journal of Geotechnical and Geoenvironmental Engineering, ASCE*. 128(9): 756-763.

Tsaparas I., Rahardjo, H., Toll D.G. and Leong E.C. (2002). Controlling Parameters for Rainfall-Induced Landslides. *Comput. and Geotech*. 29: 1-27.

Van Genuchten, M.T. (1980). A closed-form equation for predicting the hydraulic conductivity of unsaturated soils. *Soil Science Society of America Journal*. 44: 892–898.

Wang, Z., Tuli, A. and Jury,W.A. (2003). Unstable Flow during Redistribution in Homogeneous Soil. *Vadose Zone Journal*. 2: 52-60.

Zhan, T.L.T. and Ng, C.W.W. (2004). Analytical Analysis of Rainfall Infiltration Mechanism in Unsaturated Soils. *International Journal of Geomechanics, ASCE*. 4(4): 273-284

# APPENDIX A

## APPENDIX A

## Program for CR10X Data Logger

```
;{CR10X}
;Program Name: cr10x_program
;Date: 29th January 2007
;
;This program will monitor
;32 x 5301 Pressure Transducers (connected to Jetfill Tensiometer) 4-20mA output. 0-100kPa (0-1 bar) range
;32 x 5201f1L06 Gypsum Moisture Block
;---------------------------------------------------------------------
;Wiring for 5301 Pressure Transducers (qty 32)
; CR10X - AM416#1
;-----------------
; C1       - RES
; C2       - CLK
; 12V      - 12V
; G        - G

; SE1      - COM H1
; SE2      - COM L1
; SE3      - COM H2
; SE4      - COM L2

;SE2 loop to G
;SE4 loop to G
;100 Ohm precision resistor needs to be wired between SE1 and SE2
;100 Ohm precision resistor needs to be wired between SE3 and SE4

;Channel 1 on AM416
;-------------------
;Sensor#1    - AM416#1
; White       - H1
; Green       - L1
;Sensor#2 - AM416#1
; White       - H2
; Green       - L2
;Repeat the above for each of the 16 channels on the AM416.
; Relay
; C8
; G
```

;Note: The Pressure Transducers require a independent 24V power supply. The power supply is to be connected to the sensors via a relay (see wiring above)
; The ground for the sensor power supply and the CR10X power supply need to be linked.

```
;-----------------------------------------------------------------------
;Wiring for the 5201f1L106 Gyspsum Blocks (qty 32)
; CR10X - AM416#2
;-----------------------------------
; C3       - RES
; C4       - CLK
; 12V      - 12V
; G        - G

; SE5      - COM H1
; AG       - COM L1
; SE6      - COM H2
; AG       - COM L2

;Channel 1 on AM416
;-------------------
;Sensor#1    - AM416#1
; Wire1       - H1
; Wire2       - L1
;Sensor#2    - AM416#1
; Wire1       - H2
; Wire2       - L2
;Repeat the above for each of the 16 channels on the AM416

; 1k Ohm resistor needs to be wired between E1 and SE5
; 1k Ohm resistor needs to be wired between E1 and SE6

;-----------------------------------------------------------------------
*Table 1 Program
   01: 10            Execution Interval (seconds) ;
;-------------------------------------------------------------
```

; Every minute, set Flag 1 to measure the sensors. Flag 1 can be set manually at any time to make measurements.

```
32:    If time is (P92)
  1: 0            Minutes (Seconds --) into a
  2: 1            Interval (same units as above)
  3: 11           Set Flag 1 High
;-----------------------------------------------------------
```

```
; If Flag 1 is high, make measurements.
4:    If Flag/Port (P91)
  1: 11            Do if Flag 1 is High
  2: 30            Then Do

;Switch relay ON to power the pressure transducers
        5:    Do (P86)
          1: 48            Set Port 8 High

  ; Turn the multiplexer#1 ON.
        6:    Do (P86)
          1: 41            Set Port 1 High

        ; Loop of 16 (w/2 reps) for 32 pressure transducer sensors.
        7:    Beginning of Loop (P87)
          1: 0             Delay
          2: 16            Loop Count

              ; Switch the multiplexer to the next channel.
              8:    Do (P86)
                1: 72            Pulse Port 2

              ; Allow a delay for switch bounce and for the sensor output to stabilize.
              9:    Excitation with Delay (P22)
                1: 3             Ex Channel
                2: 0             Delay W/Ex (0.01 sec units)
                3: 5             Delay After Ex (0.01 sec units)
                4: 0             mV Excitation

              10:    Step Loop Index (P90)
                1: 2             Step

              ;Take measurement
              11:    Volt (Diff) (P2)
                1: 2             Reps
                2: 5             2500 mV Slow Range
                3: 1             DIFF Channel
                4: 1          -- Loc [ PresKPa_1 ]
                5: 0.0625     Multiplier
                6: -25           Offset

        12:    End (P95) ; End of Loop.

        ; Turn the multiplexer#1 OFF.
```

```
        13:   Do (P86)
          1: 51          Set Port 1 Low

        ;Switch relay OFF.
        14:   Do (P86)
          1: 58          Set Port 8 Low

;Convert KPa to bar
        15:   Beginning of Loop (P87)
          1: 0           Delay
          2: 32          Loop Count

              16:   Z=X/Y (P38)
                1: 1        -- X Loc [ PresKPa_1 ]
                2: 488          Y Loc [ BarConver ]
                3: 33       -- Z Loc [ PresBar_1 ]

        17:   End (P95)


 ; Turn the multiplexer#2 ON.
        18:   Do (P86)
          1: 43          Set Port 3 High

        ; Loop of 16 (w/2 reps) for 32 pressure transducer sensors.
        19:   Beginning of Loop (P87)
          1: 0           Delay
          2: 16          Loop Count

              20:   Step Loop Index (P90)
                1: 2            Step

              ; Switch the multiplexer to the next channel.
              21:   Do (P86)
                1: 74           Pulse Port 4

              ; Allow a delay for switch bounce and for the sensor output to stabilize.
              22:   Excitation with Delay (P22)
                1: 1            Ex Channel
                2: 0            Delay W/Ex (0.01 sec units)
                3: 5            Delay After Ex (0.01 sec units)
                4: 0            mV Excitation

              ;Take measurement
```

```
            23:   AC Half Bridge (P5)
              1: 2            Reps
              2: 14           250 mV Fast Range
              3: 5            SE Channel
              4: 1            Excite all reps w/Exchan 1
              5: 250          mV Excitation
              6: 65       -- Loc [ Ohm_1        ]
              7: 1.0          Multiplier
              8: 0.0          Offset

            24:   BR Transform Rf[X/(1-X)] (P59)
              1: 2            Reps
              2: 65       -- Loc [ Ohm_1        ]
              3: 1            Multiplier (Rf)

        25:   End (P95) ; End of Loop.

        ; Turn the multiplexer#2 OFF.
        26:   Do (P86)
          1: 53           Set Port 3 Low

     ;Turn Switch 12V on for AVW1
        27:   Do (P86)
          1: 47           Set Port 7 High

;-----------------------------------------------------
;Set Output flag high and store data

28:   If time is (P92)
  1: 0            Minutes (Seconds --) into a
  2: 5            Interval (same units as above)
  3: 10           Set Output Flag High (Flag 0)


29:   Set Active Storage Area (P80)^21267
  1: 1            Final Storage Area 1
  2: 100          Array ID

30:   Sample (P70)^13475
  1: 20           Reps
  2: 1            Loc [ PresKPa_1 ]

31:   Sample (P70)^4633
  1: 20           Reps
```

```
 2: 65          Loc [ Ohm_1       ]

32:   Sample (P70)^27719
 1: 20          Reps
 2: 456         Loc [ SucKPA_1    ]

*Table 2 Program
   02: 0.0000       Execution Interval (seconds)

*Table 3 Subroutines

End Program

-Input Locations-
1 PresKPa_1 7 2 1
2 PresKPa_2 27 1 1
3 PresKPa_3 11 1 0
4 PresKPa_4 3 1 0
5 PresKPa_5 3 1 0
6 PresKPa_6 3 1 0
7 PresKPa_7 3 1 0
8 PresKPa_8 3 1 0
9 PresKPa_9 3 1 0
10 PresKP_10 3 1 0
11 PresKP_11 3 1 0
12 PresKP_12 3 1 0
13 PresKP_13 3 1 0
14 PresKP_14 3 1 0
15 PresKP_15 3 1 0
16 PresKP_16 3 1 0
17 PresKP_17 3 1 0
18 PresKP_18 3 1 0
19 PresKP_19 3 1 0
20 PresKP_20 3 1 0
21 PresKP_21 3 0 0
22 PresKP_22 3 0 0
23 PresKP_23 3 0 0
24 PresKP_24 3 0 0
25 PresKP_25 3 0 0
26 PresKP_26 3 0 0
27 PresKP_27 3 0 0
28 PresKP_28 3 0 0
29 PresKP_29 3 0 0
30 PresKP_30 3 0 0
```

31 PresKP_31 3 0 0
32 PresKP_32 19 0 0
33 Ohm_1 7 3 2
34 Ohm_2 27 2 2
35 Ohm_3 11 1 0
36 Ohm_4 11 1 0
37 Ohm_5 11 1 0
38 Ohm_6 11 1 0
39 Ohm_7 11 1 0
40 Ohm_8 11 1 0
41 Ohm_9 11 1 0
42 Ohm_10 11 1 0
43 Ohm_11 11 1 0
44 Ohm_12 11 1 0
45 Ohm_13 11 1 0
46 Ohm_14 11 1 0
47 Ohm_15 11 1 0
48 Ohm_16 11 1 0
49 Ohm_17 11 1 0
50 Ohm_18 11 1 0
51 Ohm_19 11 1 0
52 Ohm_20 11 1 0
53 Ohm_21 11 0 0
54 Ohm_22 11 0 0
55 Ohm_23 11 0 0
56 Ohm_24 11 0 0
57 Ohm_25 11 0 0
58 Ohm_26 11 0 0
59 Ohm_27 11 0 0
60 Ohm_28 11 0 0
61 Ohm_29 11 0 0
62 Ohm_30 11 0 0
63 Ohm_31 11 0 0
64 Ohm_32 19 0 0
-Program Security-
0000
0000
0000
-Mode 4-
-Final Storage Area 2-0
-CR10X ID-0
-CR10X Power Up-3

## LIST OF RELATED PUBLICATIONS

i. Gofar, N., Lee, M.L. and Kassim, A. (2006). Effect of Surface Boundary Condition on Rainfall Infiltration. *Jurnal Teknologi B, UTM*. 44.

iii. Gofar, N., Lee, M.L. and Kassim, A. (2008). Instrumented Soil Column Model for Rainfall Infiltration Study. *Proceeding, International Conference on Geotechnical and Highway Engineering (GEOTROPIKA 2008)*. 26-27 May 2008, Kuala Lumpur.